Development 127, 3815-3828 (2000)
Printed in Great Britain © The Company of Biologists Limited 2000
DEV1537



# *sucker* encodes a zebrafish Endothelin-1 required for ventral pharyngeal arch development

**Craig T. Miller[1,*], Thomas F. Schilling[2], Kyu-Ho Lee[3], Jewel Parker[1] and Charles B. Kimmel[1]**

[1]Institute of Neuroscience, 1254 University of Oregon, Eugene, OR 97403-1254, USA
[2]Department of Anatomy and Developmental Biology, University College London, Gower Street, London, WC1E 6BT, UK
[3]Cardiology Department, Children's Hospital, Boston; and Biochemistry, Cell and Molecular Pharmacology Department, Harvard Medical School, 240 Longwood Avenue, Boston, MA 02115, USA
*Author for correspondence (e-mail: miller@uoneuro.uoregon.edu)

*Accepted 20 June; published on WWW 9 August 2000*

## SUMMARY

**Mutation of *sucker (suc)* disrupts development of the lower jaw and other ventral cartilages in pharyngeal segments of the zebrafish head. Our sequencing, cosegregation and rescue results indicate that *suc* encodes an Endothelin-1 (*Et-1*). Like mouse and chick *Et-1*, *suc/et-1* is expressed in a central core of arch paraxial mesoderm and in arch epithelia, both surface ectoderm and pharyngeal endoderm, but not in skeletogenic neural crest. Long before chondrogenesis, *suc/et-1* mutant embryos have severe defects in ventral arch neural crest expression of *dHAND*, *dlx2*, *msxE*, *gsc*, *dlx3* and *EphA3* in the anterior arches. Dorsal expression patterns are unaffected. Later in development, *suc/et-1* mutant embryos display defects in mesodermal and endodermal tissues of the pharynx. Ventral premyogenic condensations fail to express *myoD*, which correlates with a ventral muscle defect. Further, expression of *shh* in endoderm of the first pharyngeal pouch fails to extend as far laterally as in wild types. We use mosaic analyses to show that *suc/et-1* functions nonautonomously in neural crest cells, and is thus required in the environment of postmigratory neural crest cells to specify ventral arch fates. Our mosaic analyses further show that *suc/et-1* nonautonomously functions in mesendoderm for ventral arch muscle formation. Collectively our results support a model for dorsoventral patterning of the gnathostome pharyngeal arches in which Et-1 in the environment of the postmigratory cranial neural crest specifies the lower jaw and other ventral arch fates.**

Key words: *sucker*, Zebrafish, Endothelin, Pharyngeal arch, Cranial neural crest

## INTRODUCTION

In all vertebrate embryos, segmental streams of cranial neural crest cells migrate to form the pharyngeal arches and differentiate into cartilages and bones of the head skeleton. In gnathostomes, the head skeleton has a dorsoventral (DV) polarity from its first appearance: dorsal and ventral cartilages of different shapes (such as the upper jaw and lower jaw in the first arch) are separated by joints. Fate-mapping studies in the avian embryo have shown that these dorsal and ventral skeletal elements arise from different anteroposterior levels of midbrain and hindbrain neural crest (Köntges and Lumsden, 1996), suggesting that before migration, the cranial neural crest is prepatterned with respect to its DV fate. Since the cranial neural crest has been shown to pattern morphogenesis of the paraxial mesodermally derived pharyngeal musculature (Noden, 1983a,b; Schilling et al., 1996), patterning information in the head periphery could be primarily contained within the premigratory neural crest. However, other experiments have established that neural crest cells are patterned by their environment after migration. For example, cartilage histogenesis of the neural crest requires contact with pharyngeal endodermal epithelium (reviewed in Hall, 1978) and chondrification of the lower jaw is inhibited by surface ectoderm (Kollar and Mina, 1991; Mina et al., 1994). Thus, pharyngeal arch development requires bidirectional signaling between the cranial neural crest and its environment.

Targeted mutations in mice have revealed a signal present in the environment of the cranial neural crest which is required for ventral neural crest-derived skeletal fates. Inactivation of genes encoding either the 21-amino-acid secreted ligand Endothelin-1 (*Et-1)*, the Endothelin type A receptor (*EdnrA)*, or the Endothelin converting enzyme *(Ece-1)*, produces an identical craniofacial phenotype in which cartilages in the first and second arches are deleted or mispatterned (Kurihara et al., 1994; Clouthier et al., 1998; Yanagisawa et al., 1998). This common phenotype of the *Et-1* and *EdnrA* mutant mice is remarkable given the complementary expression profiles of these genes in the arch primordia. While *Et-1* is expressed in a central mesenchymal core of arch paraxial mesoderm, *EdnrA* is expressed in a surrounding shell of mesenchymal postmigratory neural crest cells. *Et-1* is also expressed in epithelia (both surface ectoderm and pharyngeal endoderm) surrounding this entire concentric arrangement of mesenchyme (Maemura et al.,

1996; Clouthier et al., 1998). The germ layer derivations of the mesenchymal populations expressing these genes are inferred from fate-mapping studies, which have established that paraxial mesoderm occupies the core of an arch and is surrounded by neural crest (Trainor et al., 1994; Trainor and Tam, 1995; Hacker and Guthrie, 1998). In both *Et-1* and *EdnrA* mutant mice, skeletal defects are preceded by much earlier defects in gene expression; for instance, *dHAND*, which encodes a bHLH transcription factor, is not expressed as it normally would be in ventral arch presumptive postmigratory crest (Thomas et al., 1998). Hence, the mutant phenotypes and expression patterns suggest a model in which Et-1 in the environment of the cranial neural crest specifies ventral crest fates.

This model is further supported by work in avian embryos, which has shown that pharmacological inactivation of EDNRA results in severe ventral arch one and two deletions, creating a chicken with no lower beak (Kempf et al., 1998). As in mice, chick *Et-1* and *EdnrA* are expressed in arch cores and epithelia, and postmigratory neural crest, respectively (Nataf et al., 1998; Kempf et al., 1998). Thus, both this anatomical arrangement of *EdnrA*-expressing cylinders of neural crest cells surrounding a central core of *Et-1*-expressing paraxial mesoderm and a required function for EDNRA in lower jaw development have been conserved between birds and mammals and, thus, likely date back at least 350 million years to the Carboniferous, the time of the last common ancestor of both mammals and the diapsids from which birds derive. The appearance of jaws earlier in vertebrate evolution, around 450 million years ago in the Ordovician, sparked the gnathostome radiation, which generated most of the vertebrates alive today (reviewed in Mallatt, 1997). The conservation of *Et-1* signaling for lower jaw development in chicks and mice raises the possibility that *Et-1*'s requirement for lower jaw development is much more ancient and shared within all gnathostomes. If so, *Et-1* should be required for lower jaw development in the most divergent gnathostomes, sharks and bony fish.

Genetic screens in the zebrafish have revealed a large number of loci required for pharyngeal arch development (reviewed in Schilling, 1997). Four recessive loci isolated in the Tübingen screen were placed into a single phenotypic class based on their similar mutant phenotypes (Piotrowski et al., 1996; and see Discussion). *sucker* (*suc*) mutants have the most severe phenotype of the four: the lower jaw and other ventral cartilages are drastically reduced, misshapen and fused to the relatively unaffected dorsal cartilages of the same arch (Piotrowski et al., 1996; Kimmel et al., 1998).

Here we present molecular and phenotypic characterization of *suc*. We show that a missense mutation in the secreted domain of an *et-1* ortholog cosegregates with the *suc* mutant phenotype, and wild-type, but not mutant, *et-1* rescues *suc* mutants. Together these results indicate that the *suc* mutant phenotype is due to this mutation in *et-1*. Injection of human ET-1 into an arch at stages after neural crest has migrated also rescues the *suc* mutant phenotype; thus, *suc/et-1* is not required for migration of most, if not all, neural crest. Rather, *suc/et-1* is required in the postmigratory environment of the neural crest where, like chick and mouse *Et-1*, *suc/et-1* is expressed in arch cores and epithelia. Zebrafish, like mice, require *et-1* signaling for the ventral arch expression of *dHAND, msxE, gsc* and *dlx3*. We find that ventral expression of *dlx2* and *EphA3* also requires *suc/et-1*, while dorsal domains of *dlx2* and *gsc* are *suc/et-1*-independent. Patterning of cranial mesodermal and endodermal tissues also requires *suc/et-1* since ventral premyogenic condensations, ventral pharyngeal muscles and the hyomandibular pouch are all mispatterned in *suc/et-1* mutants. With mosaic analyses, we demonstrate that *suc/et-1* is nonautonomously required in cranial neural crest cells for both early *dHAND* and *EphA3* expression, and for later formation of ventral pharyngeal cartilages. *suc/et-1* is also nonautonomously required in mesoderm to make correctly patterned ventral muscles. Our findings show that Et-1 signaling plays an essential role in lower jaw formation, which has been widely conserved within gnathostomes. Further, the results support a model in which the signaling occurs during a conserved transient anatomical arrangement: hollow neural crest cylinders surround central cores of paraxial mesoderm, and ventral neural crest requires Et-1 from its surrounding environment to make a lower jaw and other ventral arch fates.

## MATERIALS AND METHODS

### Maintenance of fish

Fish were raised under standard conditions (Westerfield, 1995) and staged as described (Kimmel et al., 1995). *suc*$^{tf216b}$ mutants (Piotrowski et al., 1996) were outcrossed to the Oregon ABC strain for phenotypic analyses. For some of the analyses at larval stages, mutants were outcrossed to *golden* (*gol*) (Streisinger et al., 1981) to obtain double mutant embryos with reduced pigmentation. No additional phenotypic differences were observed between *suc* mutants and *suc; gol* double mutants.

### Tissue labeling procedures

Cartilage staining, dissection and flat-mounting were done as described (Kimmel et al., 1998).

In situ hybridization was performed essentially as described (Thisse et al., 1993) with the following modifications: probes were not hydrolyzed, the glycine stop step was omitted, hybridization temperature was 66.5°C, two 30 minute 0.1× SSC washes were done after the 0.2× SSC washes, and older embryos were permeabilized by treating with 10 μg/ml Proteinase K treatment for 1 to 30 minutes depending on age. Probes used were: *dlx2* and *dlx3* (Akimenko et al., 1994), *dHAND* (Angelo et al., 2000), *msxE* (Ekker et al., 1997), *gsc* (Schulte-Merker et al., 1994), *EphA3* (Xu et al., 1995), *MyoD* (Weinberg et al., 1996), and *shh* (Krauss et al., 1993). For *suc/et-1* in situs, probe was made from EST clone fb14d01 (see below). Deyolking was done manually with tungsten insect pins. Embryos were cleared in 70% glycerol, mounted on bridged coverslips and photographed on a Zeiss Axiophot microscope. Occasionally, embryos were raised in 0.003% PTU (1-phenyl 2-thiourea) to inhibit melanogenesis (Westerfield, 1995). Two-color in situs were done as described (Jowett and Lettice, 1994) with the modifications of Hauptmann and Gerster (1994) and the same modifications as above. For sectioning, embryos were embedded in Epon and sectioned at 5 μm.

Larval muscles were stained with the 1025 anti-myosin antibody (generous gift of Drs S. Hughes and H. Blau) as described by Schilling and Kimmel (1997).

### Mapping

We mapped *suc* to LG19 using a single large early pressure (EP)-derived gynogenetic clutch (Streisinger et al., 1981) obtained from a *suc* heterozygous female, which was generated by crossing *suc* heterozygotes to the WIK mapping strain (Knapik et al., 1996). Of 95 total diploid animals, 18 were by morphology *suc* mutants. DNA was prepared from each of these animals essentially as described (Johnson

et al., 1994) and used for centromere linkage analysis (Johnson et al., 1996) with mapped z-markers and gene RFLPs (Knapik et al., 1998; Postlethwait et al., 1998) using PCR conditions as described (Johnson et al., 1994).

### Cloning *endothelin-1*

EST clone fb14d01 (M. Clark and S. Johnson, WUZGR; http://zfish.wustl.edu) was purchased from Research Genetics. This clone contains a 563 bp ORF of a zebrafish *Endothelin-1* gene (GenBank accession number AF281858). Using gene-specific primers 5′-GTGACCACAGAAATGGCGATTA-3′ and 5′-TCTGCA-ATCAGGGACTCTAG-3′ from the sequence of this EST, we screened a PAC library (Amemiya and Zon, 1999) by PCR (3 minute denaturation at 94°C followed by 37 cycles of 20 second 94°C denaturation, 20 second 53°C annealing, 30 second extension at 72°C). All PCR reactions were done on a MJ Research PTC-100 or PTC-200 using conditions essentially as described (Johnson et al., 1994). A single PAC, 16A1, was isolated which contained all five exons spanned by this EST. cDNAs were obtained from clutches of *suc* mutant embryos by RT-PCR. Total RNA was isolated using standard methods (Chomczynski and Sacchi, 1987). Primer 5′-CCTGAAATGCATGACGTGTG-3′ was used for first-strand cDNA synthesis using Superscript II reverse transcriptase (Gibco). RT-PCR was done with this reverse primer and forward primer 5′-AATACGGGACTTGCATACTACA-3′ (3 minute 94°C denaturation, followed by 36 cycles of 15 second denaturation at 94°C, 15 second annealing at 56°C, 1 minute extension at 72°C). These 659 bp RT-PCR products were cloned with a TOPO TA kit (Invitrogen) into pCR2.1, and this wild-type cDNA clone is referred to as pET1. All sequencing was done on an ABI automated sequencer.

### Rescue experiments

For DNA injections, DNA was diluted in 0.2 M KCl and 0.25% Phenol Red and pressure-injected asymmetrically into the yolk at the 2- to 4-cell stage. A 677 bp *Eco*RI fragment of pET1 (wild-type *Et-1* cDNA), containing 69 bp upstream of the predicted ATG start codon and 65 bp downstream of the predicted stop codon, was subcloned into the *Eco*RI site of pCS2, to make pCS2-ET1. Injecting this construct allows unambiguous genotyping of injected animals with intronic primers flanking the *et-1 Mse*I RFLP, since the intronic primers do not amplify the injected wild-type cDNA. Point mutagenesis was done on pCS2-ET1 using Promega's Gene Editor Site-Directed Mutagenesis kit and mutagenic primer 5′-GCAAGTTTTCTGG**T**TAAAGAGTGCGTCTAC-3′ (mismatch in bold) to create pCS2-ET1D8V. Injected animals were screened at 4 days for head morphology, and all potentially rescued mutants were anesthetized, sacrificed and bisected, their heads fixed for Alcian staining of cartilages and their tails used for making DNA for PCR-genotyping with primers 5′-GCGACAAATTCAATCATCTCTAG-3′ and 5′-ACAGTTCATAACTGATGGTATTTG-3′. A PCR program of an initial 3 minute 94°C denaturation, followed by 35 cycles of a 20 second 94°C denaturation, a 15 second 55°C annealing, and a 25 second 72°C extension generates a 300 bp band, which, when digested with *Mse*I, allows genotyping for the Asp-to-Val polymorphism (see Fig. 2E,F). Since injected DNA is inherited mosaically (see Westerfield et al., 1992; Kroll and Amaya, 1996), only a fraction of animals injected with this construct have expression driven in the head (data not shown).

For protein rescue, human recombinant mature ET-1 (Sigma) was diluted in distilled water (0.5 mg/ml) and pressure-injected into pharyngeal arch primordia through a glass micropipette using a picospritzer (Applied Instruments). Injected embryos were raised to 4 days for Alcian staining of head cartilages and PCR-genotyping of tails as described above.

### Mosaic analyses

*suc* mutant heterozygous carriers were intercrossed and donor embryos labeled at 1- to 2-cell stages with 3% biotinylated dextran. Cells were transplanted into unlabeled sibling hosts either at late blastula (mesoderm) or 3 to 5 somites (neural crest), by mounting them in 3% methyl cellulose and transferring cells using a suction micropipette as described previously (Hatta et al., 1990 for mesoderm transplants; Schilling et al., 1996 for crest transplants). Donor cells were detected with an ABC kit (Vectostain) using either a DAB substrate, or a tyramide substrate, which was detected by fluorescence (Moens and Fritz, 1999). Images were captured on a Zeiss Axioplan 2 fluorescence microscope using a CCD camera and Macintosh G3 equipped with Improvision imaging software.

## RESULTS

### Ventral cartilage defects in *sucker* mutants

*sucker* (*suc*) is one of a class of four mutations that disrupts patterning in the two anteriormost pharyngeal arches, the mandibular and hyoid. In homozygous *suc* mutant larvae, ventral cartilages (Meckel's cartilage in the mandibular arch and the ceratohyal in the hyoid) are severely reduced and fused to the dorsal cartilages of the same arches (Fig. 1, Piotrowski et al., 1996; Kimmel et al., 1998). Quantification of this phenotype shows that the expressivity of severe ventral reductions in the first two arches is 100% in *suc* mutants (Table 1). The ventral cartilages in arches 3 and 4 are also dramatically reduced with high expressivity in *suc* mutants, while cartilages in the three most posterior arches are spared (Table 1).

### A mutation in an *endothelin-1* ortholog cosegregates with *sucker*

The ventral pharyngeal cartilage reduction seen in *suc* mutants is reminiscent of the phenotype seen in mice with targeted mutations in *Endothelin-1 (Et-1)*, where homologous ventral (distal) skeletal elements (such as Meckel's cartilage) are dramatically reduced (Kurihara et al., 1994). As an initial step towards the molecular identification of the *sucker* locus, we mapped *suc* to linkage group 19 (LG19) (Fig. 2A), distal to three previously mapped zebrafish genes that are homologs of human genes on chromosome 6 (Fig. 2B). In humans, *ET-1* maps to chromosome 6, distal to the syntenic region described above (Fig. 2B). Based on the phenotypic similarities between the *Et-1* mutant mice and *suc* mutants, as well as this potential synteny, we tested a zebrafish *et-1* as a candidate for *suc*. An EST

**Table 1. Ventral cartilage defects in *suc* mutants**

| Arch | % Severe ventral reductions |
|---|---|
| 1 (mandibular) | 100 (100/100) |
| 2 (hyoid) | 100 (100/100) |
| 3 | 100 (100/100) |
| 4 | 94 (94/100) |
| 5 | 4 (4/100) |
| 6 | 0 (0/100) |
| 7 | 0 (0/100) |

100 mutants from 3 clutches (uninjected siblings of injected fish in Table 2) were Alcian stained and scored for ventral cartilage. Severe reductions were defined as both ventral cartilages being less than half the size of their wild-type counterparts (as in Figs 1D and 3B). In mutants, ventral cartilage was defined as cartilage attached to the dorsal cartilage, and in all mutants, joints were absent in both arch one and two. In addition to this ventral cartilage, each mutant had from 1-7 small ectopic ventral cartilages (see Fig. 3D; and Piotrowski et al., 1996), including at least one in the position of the basihyal (but never a correctly patterned basihyal), and each had, on average, 3.7 ectopic cartilage nodules in the anterior arches.

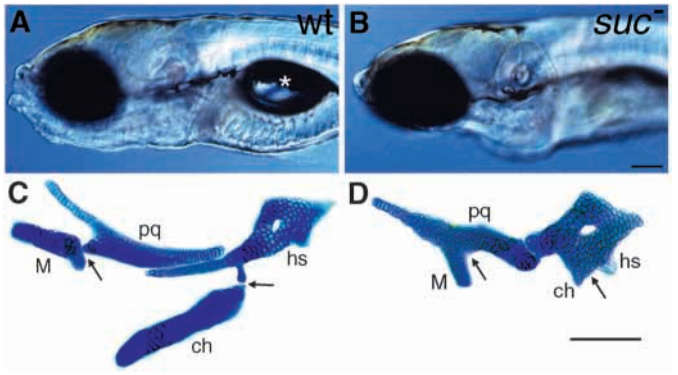


**Fig. 1.** *suc* mutants have reduced ventral cartilages. (A,B) Lateral views of live wild-type (A) and *sucker* mutant (B) larvae at 4 days. Mutants lack lower jaws and do not form swim bladders (asterisk in A). (C,D) Alcian-stained cartilages from a wild type (C) and *suc* mutant (D) dissected from the arches and flat-mounted. In wild types, dorsal and ventral elements in the first arch (pq, palatoquadrate; M, Meckel's) and second arch (hs, hyosymplectic; ch, ceratohyal) are separated by joints (arrows). In mutants, ventral cartilages are reduced and fused to dorsal cartilages at what we interpret to be the sites of the missing joints (arrows). Scale bars: 100 μm.

encoding a predicted protein highly similar to mammalian ET-1 (Fig. 2C) was generated by Washington University Zebrafish Genome Resources (http://zfish.wustl.edu) and mapped close to *suc* on LG19. Eighteen of the 21 amino acids in the predicted secreted domain are conserved between human and zebrafish (Fig. 2C,D). Sequencing of the *et-1* cDNA and genomic coding regions in *suc* mutant embryos revealed a missense mutation which replaces aspartate with valine at the highly conserved 8th residue of the 21 amino acid secreted domain (Fig. 2D,E). This transversion creates a *Mse*I site, which cosegregated with the *suc* phenotype in over 500 diploid animals (Fig. 2F and data not shown). The cosegregation places this *Mse*I RFLP and *suc* within 0.2 cM of one another, suggesting that the *suc* mutant phenotype is due to this Asp8-to-Val8 missense mutation.

## Et-1 orthologs rescue *suc* mutants

Supporting the hypothesis that *suc* is *et-1*, injection of wild-type *et-1* DNA rescued pharyngeal defects in *suc* mutants. Injection of a genomic fragment containing the entire wild-type *et-1* locus (PAC 16A1) asymmetrically into 2- to 4-cell embryos rescued ventral cartilage defects unilaterally in *suc* mutants (Table 2). Similar injections of a construct driving expression of wild-type *et-1* RNA (pCS2-ET1) also unilaterally rescued the cartilage phenotype in *suc* mutants (Fig. 3A-F and Table 2). Despite the inherent mosaicism of DNA injections (see Westerfield et al., 1992; Kroll and Amaya, 1996), injections of pCS2-ET1 rescued ventral cartilage formation in a high percentage (nearly one-quarter, Table 2; Fig. 3G) of *suc* mutants. An otherwise identical construct with the Asp8-to-Val8 missense mutation in *et-1* (pCS2-ET1D8V) did not rescue ventral cartilage formation in *suc* mutants under similar injection conditions (Table 2). These data, together with our sequencing and cosegregation results indicate that the *suc* mutant phenotype is due to this missense mutation in *et-1*, and for clarity in this paper we refer to this gene as *suc/et-1*.

The Et-1 signal might be required early for migrating precartilaginous neural crest or later within the arch primordium. To determine if Et-1 is sufficient to rescue ventral cartilage

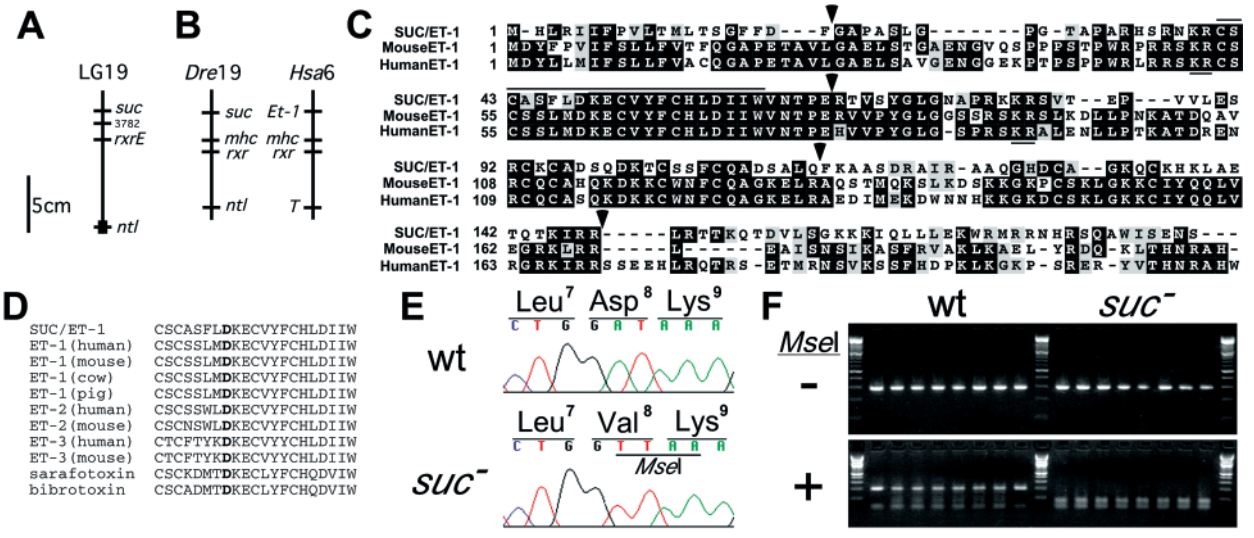


**Fig. 2.** A mutation in *et-1* cosegregates with the *suc* mutant phenotype. (A) *suc* maps to LG19. Genetic distances proximal to *suc* are reduced since half tetrads were used (Streisinger et al., 1986; see Materials and Methods). (B) Zebrafish LG19/human chromosome 6 synteny (not to scale) (Postlethwait et al., 1998; Auffrey et al., 1983; Almasan et al., 1994; Edwards et al., 1996; Hoehe et al., 1993; Gates et al., 1999). (C) Amino acid alignment of zebrafish Suc/Et-1 with human and mouse ET-1. Predicted 21-amino-acid secreted domain is overlined, dibasic residues flanking the big Et-1 domain are underlined, intron/exon boundaries of Suc/Et-1 are marked with arrowheads. (D) Alignment of 21-amino-acid secreted domains of Suc/Et-1 and other vertebrate Endothelins and two divergent asp toxins (after Janes et al., 1994). The conserved Asp8 residue is in bold. (E) Sequence of Et-1 amino acid positions 7-9 in wild type and *suc* mutant. In *suc* mutants, an A-to-T transversion results in an Asp8-to-Val8 missense mutation in *et-1*, and also creates an *Mse*I site. (F) This Asp8-to-Val8 mutation cosegregates with the *suc* mutant phenotype. Animals were sorted by jaw morphology, then genotyped for the *Mse*I RFLP by PCR using intronic primers flanking exon 2 and subsequent *Mse*I digestion (see Materials and Methods). The first and last wild-type lanes are homozygous wild types, while the middle six lanes are heterozygous for the *suc* mutant *Mse*I RFLP.

**Table 2. Et-1 rescues ventral cartilage formation in *suc* mutants**

| A. Injected DNA | DNA/embryo (pg) | % Rescue |
|---|---|---|
| PAC16A1 | 100 | 24 (13/54) |
| pCS2-ET1 | 20 | 21 (20/97) |
| | 2 | 8 (5/59) |
| pCS2-ET1D8V | 20 | 0 (0/61) |
| | 2 | 0 (0/55) |
| **B. Injected human ET-1** | **Stage** | **% Rescue** |
| | 20 hour | 28 (13/47) |
| | 28 hour | 47 (15/32) |

See Materials and Methods for description of DNA constructs and injection, genotyping, and cartilage staining protocols. Animals were considered rescued if they were homozygous *suc/et-1* mutant by PCR/*Mse*I digestion genotyping yet had ventral arch one or two cartilages (M and CH) that were correctly patterned and as large in size as their wild-type counterparts (see Fig. 3).

formation at a stage after neural crest migration, we injected human recombinant ET-1 protein into *suc/et-1* mutant arch primordia at 20 or 28 hours, two stages after most cranial neural crest has migrated (Schilling and Kimmel, 1994). Injections at both time points rescued formation of first and second arch ventral cartilages (Meckel's and ceratohyal) (Table 2, Fig. 3H). Thus, even though this experiment does not reveal the critical period when *suc/et-1* normally functions, it suggests that Et-1 is not required for ventral neural crest migration, but rather for correct specification of ventral postmigratory neural crest.

### *suc/et-1* is expressed in cores of arch mesenchyme and arch epithelia

To determine the spatiotemporal profile of embryonic *suc/et-1* expression, we examined *suc/et-1* mRNA distribution by whole-mount in situ hybridization. Whereas cranial neural crest first begins to migrate at about 12 hours in zebrafish (Schilling and Kimmel, 1994), *suc/et-1* expression in the head periphery was not detected until 16-18 hours. At this stage, small bilateral groups of mesenchymal cells adjacent to the midbrain and hindbrain express *suc/et-1* (Fig. 4A,B). Expression persists in mesenchymal cells in this location at 24 hours and, by this time, appears segmental, with one *suc/et-1*-expressing cluster of cells in each of the first two arches (Fig. 4C). At this stage, expression is also detectable in ventral pharyngeal endodermal epithelia of the second and third pharyngeal pouches (Fig. 4C) and in ventral surface ectodermal epithelium (data not shown).

In each of the first two arches at 30 hours, the *suc/et-1*-expressing mesenchyme has coalesced into a discrete cluster located ventrally (Fig. 4D). Ventral views and horizontal sections show that these mesenchymal clusters lie in a central 'core' position (Fig. 4E,F; see Introduction). By 30-32 hours, a mesenchymal cluster of *suc/et-1*-expressing cells is also detected in the core of arch 3 (Fig. 4D,F). These arch mesenchymal cores of *suc/et-1*-expressing cells are surrounded by non-expressing mesenchymal cells (Fig. 4E,F), which by position appear to be neural crest (see below). Epithelial expression persists and, at 30 hours, expression is present in pharyngeal pouches 2 and 3 and is now detected in the fourth pharyngeal pouch (Fig. 4D). At these stages, *suc/et-1* expression in ventral surface ectoderm appears continuous with expression in the pharyngeal pouches (Fig. 4F).

At 36 hours, the ventral mesenchymal cores of the arches continue to express *suc/et-1* and appear to have elongated in the mediolateral direction (Fig. 4H). Epithelial expression in both ventral surface ectoderm and pharyngeal pouches 2-4 is still detectable at this stage (Fig. 4G). Within the pharyngeal pouches, expression is restricted to posterior, ventral epithelia (Fig. 4G).

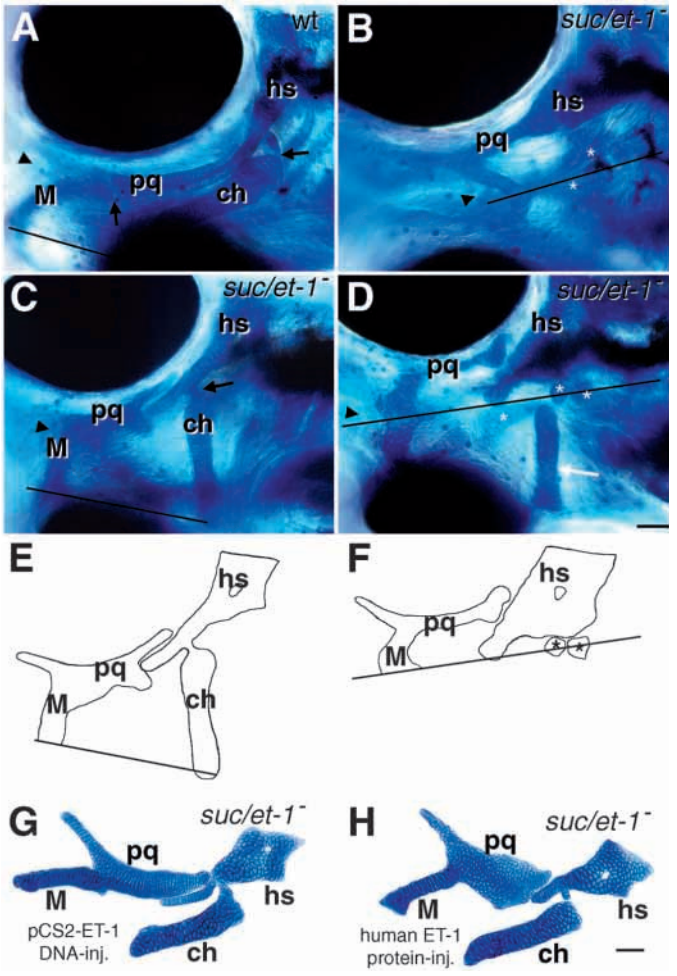


**Fig. 3.** Exogenous *et-1* rescues ventral cartilage formation in *suc* mutants. (A-D) Ventral/oblique views of Alcian-stained larvae. In all panels, the black line marks the midline, the arrowhead marks the mouth, and white asterisks mark small ectopic elements (see Table 1). Dorsal and ventral cartilages are labeled as in Fig. 1 and joints are marked with arrows. (A) Uninjected wild type. Cartilages and joints are clearly identifiable (compare to Fig. 1C and D). (B) Uninjected *suc* mutant. Ventral cartilages are reduced, joints are absent, and the mouth is displaced ventrally. (C) pCS2-ET1 DNA-injected (20 pg) PCR-genotyped *suc* mutant (rescued left side). Ventral cartilages are present unilaterally, the mouth is no longer ventrally displaced, and the second arch joint has been partially rescued. (D) Unrescued right side of animal in C. This image has been vertically flipped for comparison with A-C. Ventral cartilages on the unrescued side are severely reduced while a ceratohyal (white arrow) is present on the contralateral rescued side. (E,F) Tracings of the cartilages in C and D, respectively, labeled as in A-D. (G,H) Dissected out and flat-mounted cartilages (labeled as in Fig. 1) from the rescued side of *suc/et-1* mutants injected with 20 pg of pCS2-ET1 DNA (G) and human mature ET-1 protein (H) at 28 hours. Genotypes of all animals in C-H were confirmed by PCR-genotyping (see Materials and Methods). Scale bars, 50 μm.

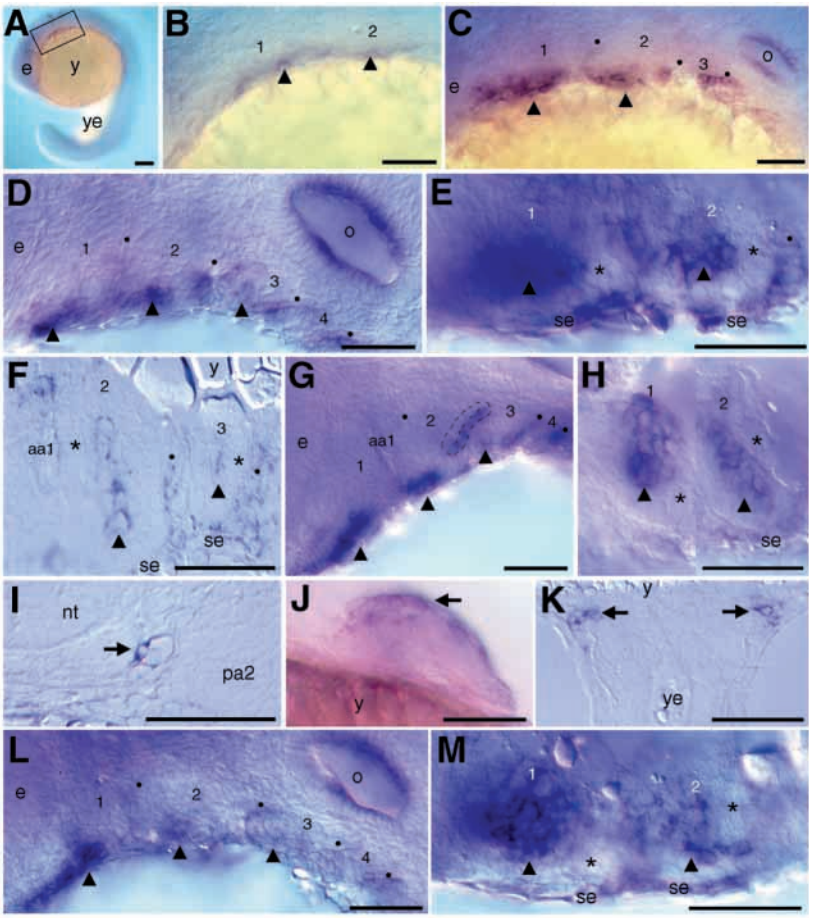


**Fig. 4.** *suc/et-1* expression in wild-type (A-K) and *suc/et-1* mutant (L,M) embryos. In all panels, when visible, the arches are numbered, arch cores are marked with arrowheads, and black dots mark the pharyngeal pouches. (A) Lateral view of a whole-mount embryo at 18 hours. (B) Higher magnification of boxed area in A. Scattered ventral mesenchymal cells in the first two arches express *suc/et-1* (arrowheads). (C) Lateral view at 24 hours. Strong expression is seen in a ventral mesenchymal cluster of cells in each of the first two arches. Expression is also seen in the second and third pharyngeal pouches. (D) Lateral view at 30 hours. Expression is seen in a mesenchymal core in each of the first three arches and in pharyngeal pouches 2-4. (E) Ventral views at 30 hours and (F) horizontal section at 32 hours through arches 2 and 3. The mesenchymal clusters of *suc/et-1*-expressing cells are surrounded by non-expressing cells (asterisks). Expression in the ventral surface ectoderm is continuous with expression in the second pharyngeal pouch. (G) Lateral view at 36 hours. Strong expression persists in a central core in the first three arches, and in pharyngeal pouches 2-4. A dashed line outlines the second pharyngeal pouch instead of marking it with a dot here to show the double cuboidal epithelial nature of the pouches, and the localization of *suc/et-1* expression to ventral, posterior pouch epithelia. (H) A montage of two focal planes of the same whole-mount embryo (ventral view) at 36 hours. The mesenchymal cores continue to express *suc/et-1* and have elongated in the mediolateral direction. (I) 32 hours; transverse section of endothelial cell (arrow) lining the dorsal aorta. (J) Ventral/lateral view of pectoral fin at 48 hours,. Anterior cells (arrow) express *suc/et-1*. (K) Horizontal section through yolk/hindyolk boundary showing bilateral clusters of *suc/et-1* expressing cells (arrows) at 24 hours. (L-M) Lateral (L) and ventral (M) views of *suc/et-1* expression in PCR-genotyped *suc/et-1* mutants at 30 hours. Both epithelial domains are present, as are strongly expressing mesenchymal cores. Compare with D-E. aa1, aortic arch 1; e, eye; nt, neural tube; o, otic vesicle; pa2, pharyngeal arch 2; se, surface ectoderm; y, yolk ball; ye, yolk extension. Scale bars, 50 μm, except A,J (100 μm).

At 48 hours, we no longer detect *suc/et-1* expression in central arch mesenchymal domains. However, expression persists in pharyngeal pouches 2-4 and is now detected weakly in the first pharyngeal pouch (data not shown).

*suc/et-1* is also expressed in other tissues, including many associated with the developing vasculature. From 24 to 36 hours, *suc/et-1* is expressed in cells lining the paired dorsal aortas and transverse sections show many of these have an endothelial morphology (Fig. 4I and data not shown). At 48 hours, *suc/et-1* expression was detected in cells lining blood vessels around the eye and in the midbrain (data not shown).

*suc/et-1* expression is also detectable in cells in the otic vesicle from 24 to 48 hours (Fig. 4C,D, data not shown), in anterior cells of the pectoral fin rudiment at 48 hours (Fig. 4J), and in discrete bilateral clusters of cells adjacent to the boundary of the yolk ball and yolk extension at 24 hours (Fig. 4K).

In PCR-genotyped *suc/et-1* mutants, the onset of *suc/et-1* mRNA expression at 18 hours appears normal and expression is detectable through 48 hours, although the expressing tissues are disorganized at later stages. At 30 hours in *suc/et-1* mutant embryos, the mesenchymal core domains express *suc/et-1*, as does both ventral surface ectoderm and pharyngeal pouches 2-4 (Fig. 4L,M). Expression in other tissues such as the otic vesicle is also not noticeably reduced in *suc/et-1* mutant embryos (Fig. 4L and data not shown).

### *suc/et-1* is required for ventral, but not dorsal, postmigratory neural crest cell fates

Since the pharyngeal cartilages affected in *suc/et-1* mutants are derived from cranial neural crest (Schilling and Kimmel, 1994), we analyzed expression of neural crest markers to determine at what stage this population is mispatterned in *suc/et-1* mutant embryos. Early stages appear normal: three markers of presumptive premigratory cranial neural crest, *fkd6* (Odenthal and Nüsslein-Volhard, 1998), *sna2* (Thisse et al., 1995) and *dlx2* (Akimenko et al., 1994) showed no defect in *suc/et-1* mutants from 10-14 hours (data not shown).

Two genes encoding transcription factors that are required for pharyngeal arch development in mice and expressed in postmigratory cranial neural crest are *dlx2* and *dHAND* (Qiu et al., 1995; Thomas et al., 1998). In wild-type zebrafish, orthologs of these genes are also expressed in postmigratory arch crest (Akimenko et al., 1994; Angelo et al., 2000). *dHAND* expression is confined to a ventral subset of *dlx2*-expressing cells (Fig. 5A). Horizontal sections of *dlx2* expression at 28 hours reveal that, within each arch, *dlx2*-expressing cells surround a central core of non-expressing cells (Fig. 5B). Similarly, viewing whole-

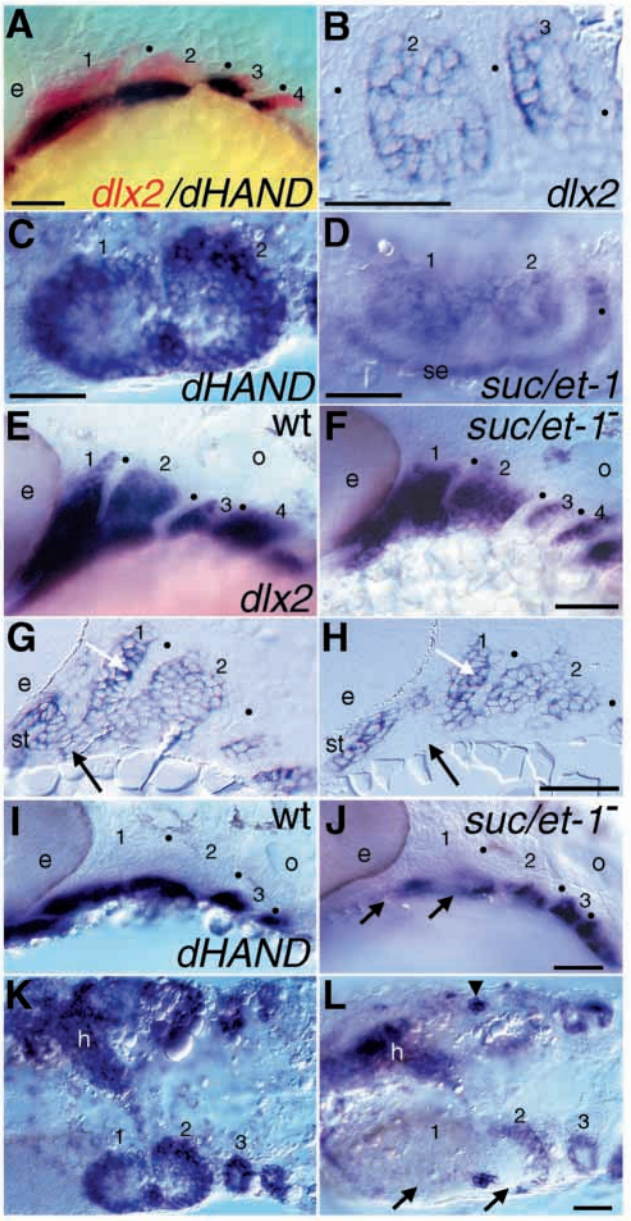


**Fig. 5.** *dlx2*, *dHAND*, and *suc/et-1* expression in wild-type (A-E,G,I,K) and *suc/et-1* mutants (F,H,J,L). In all panels, arches are numbered and when visible, the pharyngeal pouches are marked with black dots. (A) Two-color in situ hybridization with *dlx2* in red and *dHAND* in dark blue in a wild-type embryo at 28 hours. At this stage, *dHAND* expression marks a ventral subset of *dlx2*-expressing mesenchymal cells in each of the first four arches. (B) *dlx2* expression in horizontal section through arches 2 and 3 at 28 hours. Within each arch, *dlx2*-expressing cells surround a core of non-expressing cells. (C) Ventral view of *dHAND* expression in whole-mount embryo at 28 hours. Within each arch, *dHAND*-expressing cells also surround a central core of non-expressing cells. (D) Ventral view at 28 hours showing *suc/et-1* expression, which is strikingly complementary to *dHAND* expression (compare with C). *suc/et-1* expression is detected in a central core of mesenchymal cells in the first two arches, and in arch epithelia, both ventral surface ectoderm and the second pharyngeal pouch. (E-F), Lateral views, at 28 hours, of *dlx2* expression in PCR-genotyped wild-type (E) and *suc/et-1* mutant (F) whole-mount embryos. In wild types *dlx2* is expressed broadly in most if not all postmigratory arch neural crest, and is not expressed in the pharyngeal pouches. *suc/et-1* mutant embryos have a reduction of ventral *dlx2* expression. (G-H) 28 hours; sagittal sections of *dlx2* expression in PCR-genotyped wild-type (G) and *suc/et-1* mutant (H) cut through the lateral aspect of arches 1 and 2. In *suc/et-1* mutant embryos, ventral cells are present but do not express *dlx2* (black arrows). In contrast, *suc/et-1* mutant dorsal cells (white arrows) and cells lining the stomodeum express *dlx2* at normal levels. (I-L) *dHAND* expression in whole-mount wild-type (I, K) and *suc/et-1* mutant (J,L) embryos at 28 hours. I and J are lateral views, K and L are ventral views. *dHAND* expression in *suc/et-1* mutants is severely reduced in the first two arches (arrows in J and L). *dHAND* is also normally expressed in the heart, the pectoral fin (data not shown), and a discrete cluster of cells at the arch one/two boundary (arrowhead in L); these domains are not affected in *suc/et-1* mutants (K-L and data not shown). e, eye; h, heart; o, otic vesicle; se, surface ectoderm; st, stomodeum. Scale bars: 50 μm.

mount embryos from a ventral aspect reveals that, in each arch, *dHAND*-expressing cells are also arranged cylindrically and surround a non-expressing core of cells (Fig. 5C). Ventrally, *dHAND* expression is strikingly complementary to *suc/et-1* expression: core mesenchyme expresses *suc/et-1* but not *dHAND*, and peripheral mesenchyme expresses *dHAND* but not *suc/et-1* (Fig. 5C,D). The surrounding epithelia (both ventral surface ectoderm and pharyngeal endoderm) also express *suc/et-1*, but not *dHAND* (Fig. 5D).

No *dlx2* expression defect was detected in *suc/et-1* mutants at early premigratory stages (see above). However, by 28 hours, we could unambiguously sort mutants (verifying genotypes by PCR, see above) by a reduction in the dorsoventral length of the *dlx2* expression domains in the mandibular and hyoid arches (Fig. 5E,F). Dorsal cells in *suc/et-1* mutant arches express *dlx2* at normal levels (Fig. 5E,F). Hence the reduction is of the ventral domain, due to either an absence of cells ventrally, or a failure of ventral cells to express *dlx2*. The latter appears to be the case, since in sections of *dlx2* expression in *suc/et-1* mutants, ventral first and second arch crest cells appear to be present but fail to express *dlx2* (Fig. 5G,H). In accord with this interpretation, in *suc/et-1* mutants, unlabeled mesenchymal cells surround the *suc/et-1*-expressing cores (Fig. 4M). Furthermore, preliminary TUNEL labeling (data not shown) revealed no significant cell death in the arches of *suc/et-1* mutants. Therefore three lines of evidence suggest that postmigratory neural crest cells are present in the ventral arches of *suc/et-1* mutants.

*dHAND* arch expression is severely reduced in the *Et-1* mutant mice (Thomas et al., 1998). Similarly, in zebrafish, the expression of *dHAND* in ventral arch mesenchyme is dramatically reduced in *suc/et-1* mutant embryos at 28 hours (Fig. 5I-L). Expression of *dHAND* is often maintained at a low level in the posterior half of the second arch in *suc/et-1* mutants (Fig. 5K-L), suggesting additional genes are required for arch *dHAND* expression. In wild types, while *dHAND* is also expressed in the developing heart and fin, neither of these domains are noticeably affected in *suc/et-1* mutants (Fig. 5K-L and data not shown).

Two other transcription factors, Msx1 and Gsc, are required for mammalian craniofacial development (Satokata and Maas, 1994; Yamada et al., 1995; Rivera-Perez et al., 1995). *gsc*, like *dHAND*, requires *Et-1* signaling for expression in mouse arch primordia (Clouthier et al., 1998). In contrast, *msx1* arch expression is unaffected in the *Et-1* mutant mice, although *msx1* has been indirectly shown to be downstream of *Et-1* signaling (Thomas et al., 1998; and see Discussion). To test if

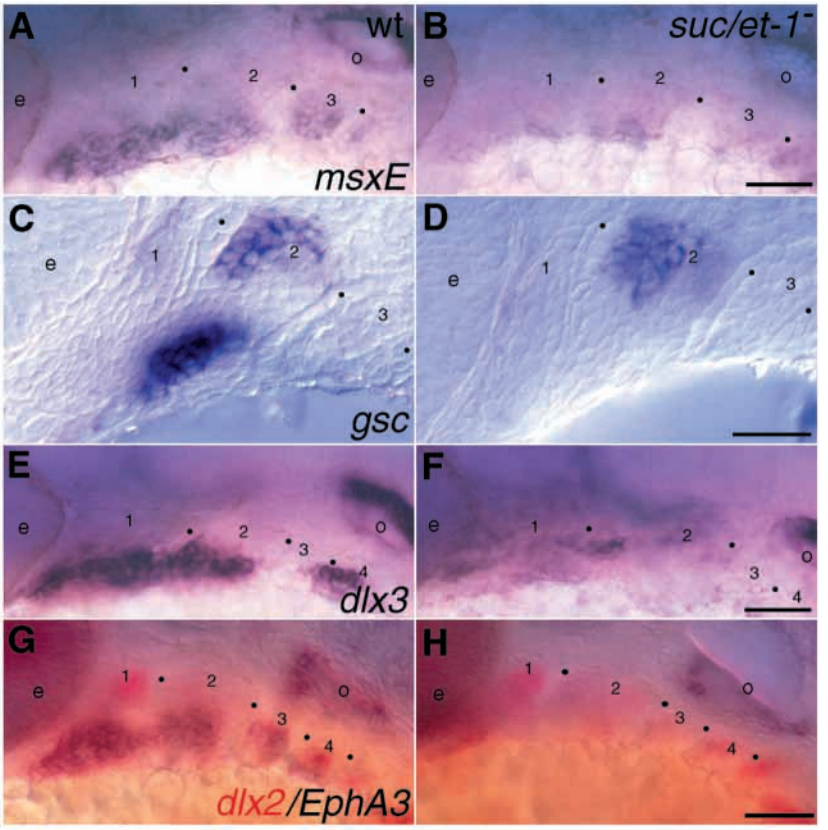


**Fig. 6.** *suc/et-1* is required for ventral neural crest specification in the arch primordia. Lateral views of whole-mount embryos processed for single color (A-F) or two-color (G,H) in situ hybridization. In all panels, the arches are numbered, and pharyngeal pouches are marked with black dots. (A-B) 24 hours, *msxE* expression in wild type (A) and *suc/et-1* mutant (B). Ventral mesenchymal cells in the first three arches express *msxE* in wild types, but do not in *suc/et-1* mutants. (C-D) 30 hour, *gsc* expression in wild type (C) and *suc/et-1* mutant (D). In wild types, *gsc* is expressed in separate patches of dorsal and ventral mesenchyme in the second arch. In *suc/et-1* mutants, dorsal cells express *gsc* while ventral cells do not. (E-F) 24 hours, *dlx3* expression in wild type (E) and *suc/et-1* mutant (F). In wild types at this stage, *dlx3* is expressed in ventral but not dorsal mesenchyme in arches one, two, and four. In *suc/et-1* mutants, ventral cells fail to express *dlx3*. (G-H) 32 hours, *dlx2* (red) and *EphA3* (blue) expression in wild type (G) and *suc/et-1* mutant (H). *EphA3* expression is ventrally restricted similar to *dHAND*. In *suc/et-1* mutants, *EphA3* expression is severely reduced in the first four arches. Fig. 5 should be referred to for the *dlx2* defect in *suc/et-1* mutants. e, eye; o, otic vesicle. Scale bars: 50 μm.

this genetic hierarchy has been conserved between fish and mammals, we examined expression of *msxE* and *gsc* in *suc/et-1* mutant embryos. In wild-type zebrafish embryos at 24 hours, *msxE* is expressed similarly to *dHAND*, in ventral but not dorsal postmigratory arch neural crest (Ekker et al., 1997; Fig. 6A). Expression in *suc/et-1* mutants is severely reduced, although other non-arch domains are unaffected (Fig. 6B).

*goosecoid* (*gsc*) expression in zebrafish marks a complex pattern of dorsal and ventral arch mesenchyme from 26-42 hours (Schulte-Merker et al., 1994; Fig. 6C and data not shown). In the hyoid arch of 30 hour wild types, these dorsal and ventral *gsc*-expressing domains of cells are separated by a non-expressing domain, which seems to prefigure the joint between the dorsal and ventral cartilages (Fig. 6C). While *gsc* is expressed dorsally in *suc/et-1* mutant embryos, ventral expression is largely abolished (Fig. 6D).

The homeobox transcription factor *dlx3* (Akimenko et al., 1994) and the ephrin receptor tyrosine kinase *EphA3* (Xu et al., 1994) are also expressed in zebrafish ventral arch postmigratory neural crest and we find that expression of both requires *suc/et-1* function (Fig. 6E-H). In wild types, arch expression of *dHAND*, *msxE*, *dlx3*, and *EphA3* are all initiated from 18-24 hours, well after *dlx2* (Ekker et al., 1997; Akimenko et al., 1994; data not shown). Defects in *msxE*, *dlx3* and *EphA3* were detected at 24 hours, while the *gsc* defect was apparent at 26 hours, when its ventral arch expression is first initiated in wild types (data not shown). *dHAND*, *msxE*, *dlx3* and *EphA3* are all also expressed in ventral postmigratory neural crest in more posterior arches (Figs 5, 6). In *suc/et-1* mutants at 24 hours, gene expression defects are usually localized to the first two arches but, by 36 hours, severe defects are also seen in the third and fourth arches (data not shown).

### *suc/et-1* is required for cranial muscle and endodermal patterning

To assay potential requirements for *suc/et-1* in cranial development outside of the neural crest, we examined arch muscles and endodermal derivatives in *suc/et-1* mutants. In wild types, both dorsal and ventral pharyngeal muscle precursors are detectable at 54 hours by expression of *myoD* (Schilling and Kimmel, 1997). However, in *suc/et-1* mutants at the same stage, the first and second arch ventral *myoD*-expressing muscle precursors were severely reduced (Fig. 7A-D). A few scattered *myoD*-expressing cells are present in the ventral arches of *suc/et-1* mutants, but the ventral premyogenic condensations fail to form (Fig. 7B,D). In contrast, forming dorsal muscles of the mandibular and hyoid arches express *myoD* and appear unaffected in *suc/et-1* mutants (data not shown).

Differentiated ventral arch muscles are also severely reduced in *suc/et-1* mutant larvae, as determined by immunostaining of 5-day-old larvae with the 1025 antibody to muscle myosins (Fig. 7E-H). The ventral first arch muscles (intermandibularis anterior and posterior) are reduced to a few fibers that span the midline (Fig. 7F), and the ventral second arch muscles (interhyoideus and hyohyoideus) fail to extend to the midline as they do in wild types and are greatly reduced in size. In contrast to these ventral disruptions, dorsal muscles are relatively unaffected and, as normal, attach to the dorsal cartilages (Fig. 7G,H).

Defects are also present in the pharyngeal endoderm of *suc/et-1* mutants. *sonic hedgehog* (*shh*) is expressed in wild-type pharyngeal endodermal cells beginning around 33 hours (Krauss

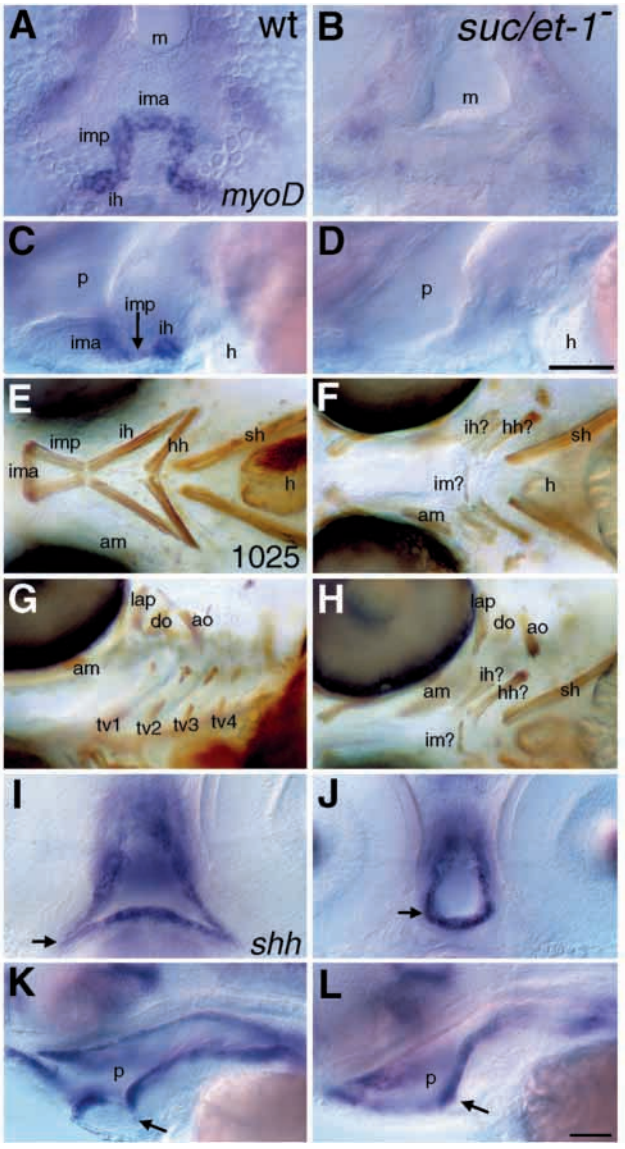


**Fig. 7.** *suc/et-1* is required for later mesodermal and endodermal patterning in the pharyngeal arches. (A-D) *myoD* expression at 54 hours in wild types (A,C) and *suc/et-1* mutants (B,D). In mutants, the mouth is displaced ventrally, and the ventral *myoD*-expressing premyogenic condensations in arches 1 and 2 are absent. (E-H) Larval muscles at 5 days detected with the 1025 antibody to muscle myosins in wild types (E,G) and *suc/et-1* mutants (F,H). In mutant larvae, ventral muscles are severely mispatterned. The first arch ventral muscles, intermandibularis anterior and posterior (ima and imp), are missing in *suc/et-1* mutants, other than a few occasional fibers spanning the midline. The ventral arch two muscles, interhyoideus and hyohyoideus (ih and hh), are dramatically shorter and do not meet in the midline as they do in wild-types (E-F). Dorsal muscles (am, lap, do, ao) appear normal in *suc/et-1* mutants. (I-L) *shh* expression in wild types (I,K) and *suc/et-1* mutants (J,L) at 54 hours. (I,J) Anterior views, focused deep to the mouth at the level of the first pharyngeal pouch, (K,L) lateral views. In mutants, expression in the first pharyngeal pouch does not extend as laterally as in wild types (arrows in I and J) and a midline diverticulum has not formed (arrows in K and L). am, adductor mandibulae; ao, adductor operculi; do, dilator operculi; h, heart; ih, interhyoideus; ima, intermandibularis anterior; imp, intermandibularis posterior; hh, hyohyoideus; lap, levator arcus palantini; p, pharynx; sh, sternohyoideus; tv1-4, branchial muscles transversus ventralis 1-4 (see Schilling and Kimmel, 1997 for wild-type muscle description). Scale bars: 50 μm.

et al., 1993), at which time no defect in *suc/et-1* mutant embryos was detected (data not shown). However, by 54 hours, a *shh* expression defect is detectable: expression in the first pharyngeal pouch does not extend as far laterally in mutants as it does in wild types (Fig. 7I,J). Furthermore, a diverticulum forming at the ventral midline of the arch one/two pharyngeal endoderm boundary, perhaps the thyroid rudiment, is visible in lateral views of 54 hour embryos but is malformed in *suc/et-1* mutant embryos (Fig. 7K,L). Thus, in addition to *suc/et-1*'s early requirement for ventral neural crest patterning, *suc/et-1* is also required to pattern later arch mesodermal and endodermal derivatives.

### *suc/et-1* functions nonautonomously in cranial neural crest for ventral arch fates and nonautonomously in mesendoderm for ventral arch muscle formation

Since ventral arch neural crest is severely mispatterned in *suc/et-1* mutant embryos, yet *suc/et-1* expression was not detected in the neural crest, we predicted neural crest cells would require *suc/et-1* function nonautonomously. To test this prediction, we performed mosaic analyses, transplanting labeled *suc/et-1* mutant premigratory cranial neural crest cells into unlabeled wild-type hosts (Fig. 8A). Neural crest cells from *suc/et-1* mutants grafted into wild-type crest at early somite stages migrated into the peripheral, *dlx2*-expressing region of the arches and, when located ventrally, expressed ventral markers such as *dHAND* and *EphA3* (Fig. 8C,E; Table 3). In similar *suc/et-1* mutant-to-wild type neural crest transplants, *suc/et-1* mutant cells also contributed to normal ventral cartilages in wild-type larvae (Fig. 8G, Table 3). Thus *suc/et-1* functions nonautonomously in the neural crest, and the skeletal defects apparently arise indirectly because of a missing signal in the crest environment.

Since we previously fate-mapped head mesoderm on the zebrafish gastrula (Kimmel et al., 1990), we could test a mesodermal role for *suc/et-1* by performing mesodermal transplants between wild-type and *suc/et-1* mutant embryos at the gastrula stage (Fig. 8B). Both wild-type and *suc/et-1* transplanted mesendodermal cells spread widely throughout the mesendoderm of a wild-type host and cells in the arches tend to occupy the central region of the arch primordium at 24 hours (Fig. 8D, data not shown), consistent with the hypothesis that paraxial mesoderm occupies the core of each arch. Transplanted cells that contributed to posterior branchial arches, which are developmentally younger, suggest that initially within the arch primordium, the neural crest is located lateral to the paraxial mesoderm (Fig. 8F).

Although these mesendodermal transplants might have contained a few pharyngeal endoderm cells, we did not observe induction of ventral neural crest markers *dHAND* or *EphA3* in *suc/et-1* mutant hosts in response to the presence of wild-type mesendoderm (Table 3). Furthermore, in the converse transplant, transplanted *suc/et-1* mutant mesodermal cells were able to form normal ventral muscles in a wild-type host (Fig. 8H, Table 3) and did not result in abnormal cartilage development. Thus, *suc/et-1* appears to also function nonautonomously in the paraxial mesoderm.

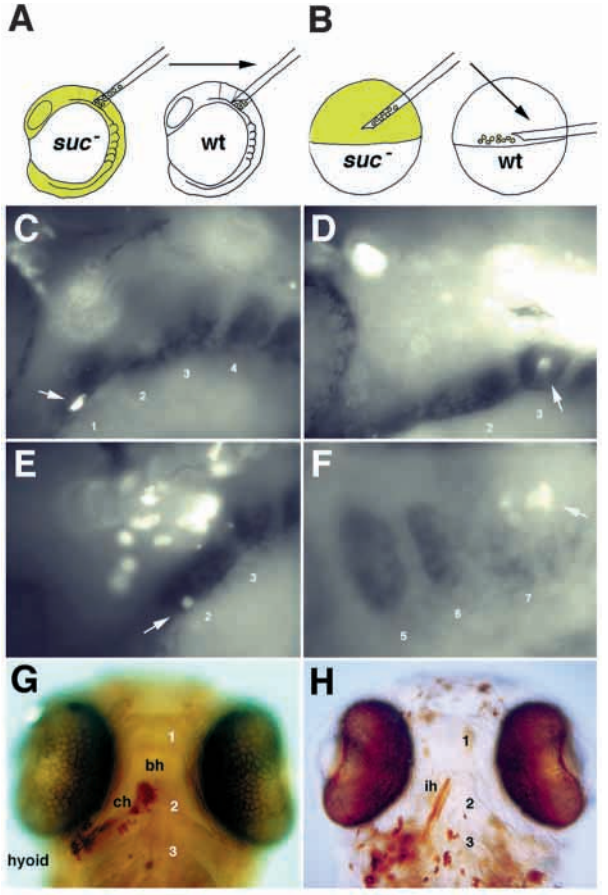


**Fig. 8.** *suc/et-1* functions nonautonomously in neural crest and mesoderm. (A) Schematic of neural crest transplants. Premigratory neural crest cells from biotin-labeled donors were tranplanted into unlabeled hosts at the 5 somite stage. (B) Schematic of mesodermal transplants. Cells from the head muscle domain of biotin-labeled gastrulas (Kimmel et al., 1990) were transplanted into the marginal region of unlabeled hosts. (C-H) Genetic mosaic animals at 24 hours (C-F) and 4 days (G,H), with the arches numbered.
(C-F) Superimposed fluorescent and bright-field images to colocalize the biotin lineage tracer with *dHAND* expression in whole-mount embryos. (C,E) *suc/et-1* mutant neural crest cells migrate into the *dHAND*-expressing region of arch one (C) and two (E). In both of these mosaic animals, *suc/et-1* mutant ventral neural crest expressed *dHAND* (see Table 3). Both wild-type (not shown) and *suc/et-1* mutant mesoderm (D) fills the non-*dHAND*-expressing central core in a wild-type host. Initially, neural crest cells lie lateral to mesoderm (F). (G) Mosaic larva in which *suc/et-1* mutant neural crest cells, labeled in brown, contributed to a normal ventral cartilage (the ceratohyal) in an unlabeled wild-type host. (H) Mosaic larva in which labeled *suc/et-1* mutant mesodermal cells have contributed to a normal ventral muscle (interhyoideus) in a wild-type host. bh, basihyal; ch, ceratohyal; ih, interhyoideus.

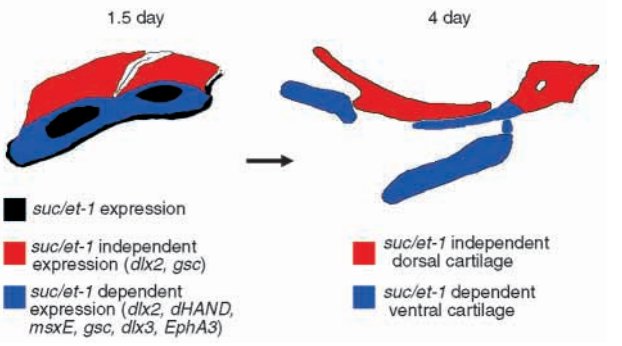


**Fig. 9.** A model for pharyngeal arch patterning. Postmigratory cranial neural crest is subdivided into dorsal (red) and ventral (blue) populations. Ventral neural crest cells require environmental *suc/et-1* (black) for expression of *dlx2*, *dHAND*, *msxE*, *gsc*, *dlx3*, and *EphA3* and later formation of ventral cartilages. Dorsal arch cores, which do not express *suc/et-1*, are not drawn. The axis we refer to as dorsoventral is sometimes called proximodistal.

## DISCUSSION

We have cloned and characterized zebrafish *sucker* (*suc*), mutation of which results in severe reduction of the lower jaw and other ventral pharyngeal arch cartilages. Our sequencing, cosegregation and rescue experiments indicate that the *suc* mutant phenotype is due to a missense mutation at a conserved residue within the secreted domain of Endothelin-1. Like mouse and chick *Et-1*, *suc/et-1* is expressed in pharyngeal arch mesenchymal cores and epithelia. These mesenchymal cores are surrounded by *dlx2* and *dHAND*-expressing putative neural crest cells, suggesting that the cores consist of paraxial mesoderm. Like mouse *Et-1*, *suc/et-1* is required for ventral arch fates, including expression of *dHAND*, *msxE*, *gsc* and *dlx3*. Additionally, in zebrafish ventral expression of *dlx2* and *EphA3* also requires *suc/et-1*. Dorsal expression of *dlx2* and *gsc* is *suc/et-1* independent, and later patterning of arch mesodermal and endodermal derivatives also requires *suc/et-1* function. Lastly, our mosaic analyses demonstrate that *suc/et-1* functions nonautonomously in both neural crest cells and paraxial mesoderm. Collectively our results support a model (Fig. 9) in which ventrally-restricted *Et-1* expression in both paraxial mesodermal arch cores and surrounding epithelia specifies ventral arch crest fates, including the ventral expression of *dlx2*, *dHAND*, *msxE*, *gsc*, *dlx3* and *EphA3* and the later formation of ventral cartilages.

**Table 3. Fates of transplanted cells in mosaic embryos**

| | Phenotypes | | Crest genes in xpl. cells | | Fates scored | |
|---|---|---|---|---|---|---|
| Transplant | Donor | Host | *dHAND* | *EphA3* | Vent. Cart. | Vent. Muscle |
| Neural crest in ventral arch | wt | wt | 100 (24/24) | 100 (13/13) | 11 (2/18) | – |
| | *suc*⁻ | wt | 44 (4/9) | 33 (1/3) | 18 (2/11) | – |
| | wt | *suc*⁻ | 0 (0/7) | 0 (0/3) | 0 (0/9) | – |
| Mesendoderm in arch | wt | wt | 0 (0/20) | 0 (0/6) | – | 20 (2/10) |
| | *suc*⁻ | wt | 0 (0/10) | 0 (0/8) | – | 10 (1/10) |
| | wt | *suc*⁻ | 0 (0/18) | 0 (0/14) | – | 0 (0/10) |

### *sucker* encodes a zebrafish Endothelin-1

Biochemical evidence indicates that the Asp8-to-Val8 missense mutation in *suc*$^{tf216b}$ is likely to be a loss-of-function mutation. Alanine scanning of the 21-amino-acid human mature ET-1 showed that Asp8 is one of only five residues which, when replaced with alanine, resulted in a nonfunctional protein (Tam et al., 1994). Hence, replacing this highly conserved charged residue of zebrafish Et-1 with a noncharged residue such as valine would be expected to create a nonfunctional protein. Our rescue experiments also suggest *tf216b* is a loss-of-function mutation, since injection of pCS2-ET1 (wild-type Et-1), but not pCS2-ET1D8V (Et-1 with Asp-to-Val missense mutation at residue 8 of secreted domain) rescued ventral cartilage formation in *suc* mutants. Further testing of the strength of the *tf216b* allele will be possible once additional alleles of *suc* are found, or a *Df(suc)* becomes available. Since *suc/et-1* is still expressed in *suc/et-1* mutants, this missense mutation does not appear to result in fewer or more unstable transcripts, and suggests that *suc/et-1* does not indirectly autoregulate its own transcription.

Mutations of three other 'anterior arch' loci (*schmerle, sturgeon* and *hoover*) cause similar craniofacial defects as those seen in *suc/et-1* mutants (Piotrowski et al., 1996). We subsequently described a common phenotypic spectrum of flat-mounted larval hyoid cartilage shapes in *sucker, schmerle* and *sturgeon* mutants and noted the resemblance of these mutant phenotypes to phenotypes seen in mice with mutations in *Et-1* signaling components (Kimmel et al., 1998). In mice, mutation of *Et-1*, *EdnrA* or *Ece-1* produces similar craniofacial defects, suggesting that, in zebrafish, some of the other anterior arch loci represent *ednrA* or *ece-1* genes, a possibility that we are currently exploring. However, the *Ece-1* mutant mice also have pigment and enteric neuron defects (Yanagisawa et al., 1998) that have not been reported for any of the zebrafish anterior arch mutants. Furthermore, the *EdnrA* and *Ece-1* mutant mice have defects in cardiac neural crest-derived tissues such as the outflow tract (Clouthier et al., 1998; Yanagisawa et al., 1998), while no circulatory system defect has been reported for any of the anterior arch mutants. Two of the other anterior arch mutations (*schmerle* and *hoover*) result in shorter pectoral fins (Piotrowski et al, 1996), which is interesting in light of *suc/et-1* expression in the developing pectoral fin. Although *suc/et-1* mutants display no obvious defects in the pectoral fin or other non-arch *suc/et-1*-expressing tissues, these tissues have not been examined comprehensively in *suc/et-1* mutants. *suc/et-1* mutants live up to 9 days, long enough to detect defects in derivatives of these *suc/et-1*-expressing tissues. These tissues in zebrafish might not require Et-1 signaling. Alternatively, the additional genomic duplication in the teleost lineage (Postlethwait et al., 1998; Amores et al., 1998) might have generated genes redundant for these developmental requirements. Redundant functions can be revealed by double mutant analyses and further motivates the isolation of more anterior arch mutants. Forward genetic screens in zebrafish could also reveal genes that have not yet been implicated in the *Et-1* signaling pathway in mice. Our ongoing head cartilage screen has uncovered a fifth anterior arch locus (C. T. M. and C. B. K., unpublished), yet no more alleles of the existing four, suggesting that the screens have not approached saturation.

### Conserved neural crest/mesodermal arrangements during gnathostome arch development

Trainor and Tam (1995) showed that, in mammalian embryos, neural crest surrounds the paraxial mesodermal core of the arch. In chick embryos, Noden (1983b) demonstrated that head paraxial mesoderm makes most of the muscles of the pharynx and Hacker and Guthrie (1998) described the migration of cranial paraxial mesoderm into the center of each pharyngeal arch. Our mosaic analyses support a neural crest origin for peripheral mesenchyme as well as a paraxial mesodermal origin for the central arch mesenchymal core.

Gene expression patterns in amniote embryos also reveal separate central and peripheral arch mesenchymal populations. In mice and chicks alike, *Et-1* is expressed in a central arch core surrounded by non-*Et-1*-expressing mesenchyme (Maemura et al., 1996; Clouthier et al., 1998; Nataf et al., 1998). In the arches of mice, *dlx2* is expressed in mesenchyme surrounding a central non-expressing core (Bulfone et al., 1993). We show that, in zebrafish, *suc/et-1* is expressed in central arch mesenchyme, while *dlx2* is expressed in peripheral mesenchyme. Thus, the general spatial arrangement of *Et-1* and *dlx2* expression in arch mesenchyme has been conserved between fish and amniotes. A higher resolution analysis of *dlx2* and *Et-1* expression, with serial sections and double-labeling experiments, would further test this model of distinct arch mesenchymal populations revealed by expression of these two genes. We propose that the *suc/et-1*-expressing ventral arch cores in the first two arches correspond to the premyogenic condensations intermandibularis and constrictor hyoideus ventralis, respectively, described by Edgeworth (1935). According to this proposal, *suc/et-1* expression marking ventral muscle precursors parallels *engrailed* expression marking dorsal muscle precursors (constrictor dorsalis) in the first arch (Miyake et al., 1992; Hatta et al., 1990; Edgeworth, 1935).

Together, our expression and mosaic analyses support a model (Fig. 9) in which arch postmigratory neural crest cells form a hollow cylinder surrounding central cores of paraxial mesoderm. Within each arch, ventral paraxial mesoderm expresses *suc/et-1* and is surrounded by ventral postmigratory neural crest. *dlx2* and *gsc* are expressed in both dorsal and ventral postmigratory arch crest, although only the ventral domains are *suc/et-1*-dependent. *dHAND*, *msxE*, *dlx3* and *EphA3* expression is ventrally-restricted and also requires *suc/et-1*. Both these gene expression patterns and these tissue arrangements argue for a conserved anatomical arrangement of arch mesenchyme that occurs transiently during arch development in all gnathostomes.

### Conserved genetic network of gnathostome pharyngeal arch patterning

The *Et-1* mutant mice have reduced *dHAND* arch expression while the *dHAND* mutant mice have no arch *msx1* expression, leading Thomas et al. (1998) to propose a pathway involving these three genes. Surprisingly, the *Et-1* mutant mice have normal *msx1* expression, possibly due to low levels of *dHAND* expression, which are sufficient to activate *msx1* at normal levels (Thomas et al., 1998). Our results demonstrate that, in zebrafish, both *dHAND* and *msxE* expression require *suc/et-1*. The orthologies of the five zebrafish *msx* genes and the three mammalian *msx* genes are unclear (Ekker et al., 1997).

However, since *msx2* expression in both the *Et-1* and *dHAND* mutant mice is normal (Thomas et al., 1998), we propose that, in the arches, *msxE* is the functional equivalent of mammalian *msx1* and that, in zebrafish, expression of this *msx* gene more directly requires *suc/et-1*.

In zebrafish, *gsc* expression requires *suc/et-1* ventrally, but not dorsally. Similarly, *gsc* expression is undetectable in E10.5 *EdnrA* mutant mice (Clouthier et al., 1998). Although no ventral specificity to this defect has been reported in mice, later in development, *gsc* is expressed in dorsal arch tissues (Gaunt et al., 1993) and *gsc* mutant mice have both dorsal and ventral craniofacial defects (Yamada et al., 1995; Rivera-Perez et al., 1995). Perhaps a later dorsal *gsc* expression domain in mice is homologous to the unaffected dorsal domain that we see in *suc/et-1* mutants. Alternatively, a second zebrafish *et-1* might activate dorsal *gsc* expression. A third possibility is that the *suc/et-1*-independent dorsal *gsc* domain is not homologous to any mammalian *gsc* expression domain. Regardless, the abolished ventral domains of *gsc* in *suc/et-1* mutant embryos show that, in zebrafish and mice alike, some expression of *gsc* requires *et-1*.

Interestingly, these dorsal and ventral domains of zebrafish *gsc* expression, separated by a non-expressing intermediate region, combined with ventrally restricted gene expression patterns (e.g. *dHAND)*, suggest that at this early precondensation stage, at least three arch mesenchymal fates have been specified: dorsal, intermediate or presumptive-joint, and ventral. This apparent specification of joints at a stage before they form is reminiscent of *Gdf5* expression in the mouse, which prefigures joints in the axial and appendicular skeleton (Storm and Kingsley, 1996). Since the joints between dorsal and ventral arch cartilages in *suc/et-1* mutants are also eliminated (Piotrowski et al., 1996; Kimmel et al., 1998; Fig. 1), we predict that markers discovered to be expressed in these presumptive-joint regions will be downregulated in *suc/et-1* mutants.

*dlx2* expression in cranial neural crest cells in *suc/et-1* mutant embryos is unaffected until a postmigratory stage, when ventral neural crest cells fail to express *dlx2*. Likewise, the *EdnrA* mutant mice have no early *dlx2* expression defects. However, at later stages, the *EdnrA* mutant mice fail to maintain *dlx2* expression specifically in the second arch (Clouthier et al., 2000). Thus, while these results suggest that neither fish nor mice require *et-1* signaling for early *dlx2* expression, at later stages, fish and mice require *et-1* signaling for *dlx2* expression in different subpopulations of postmigratory arch neural crest.

In zebrafish, *dlx3* arch expression is ventrally-restricted and requires *suc/et-1*. Similarly, in mice, *dlx3* arch expression is ventrally-restricted and requires *EdnrA* (Robinson and Mahon, 1994; Qiu et al., 1997; Clouthier et al., 2000). Qiu et al. (1997) suggest that the phenotypes of the *Dlx2* and *Dlx1;Dlx2* mutant mice are specific to the dorsal arches because *Dlx3* compensates for *Dlx1* and *Dlx2* ventrally. Although *Dlx3* mutant mice die too early to assess a craniofacial requirement (Morasso et al., 1999), humans with a missense mutation in *DLX3* have tricho-dento-osseous (TDO) syndrome (Price et al., 1998), which includes a craniofacial component (Kula et al., 1996).

Expression of the zebrafish ephrin receptor tyrosine kinase *EphA3* is also ventrally restricted and requires *suc/et-1*. Similarly, a mouse *EphA3* gene is expressed in Meckel's cartilage (Kilpatrick et al., 1996), although no function for *EphA3* has been demonstrated in ventral arch development. We described a ventral arch morphogenesis defect in *suc* mutants (Kimmel et al., 1998). Since all other genes thus identified as downstream of *suc/et-1* are transcription factors, *EphA3* promises to help connect this hierarchy of transcription factors with the more immediate 'effectors of morphogenesis' (Holder and Klein, 1999).

Since *dHAND, msx1* and *dlx3* are all also ventrally-restricted within mouse arches, it seems that much of the genetic network that specifies ventral arch postmigratory neural crest (Fig. 9) has been largely conserved between mice and fish. Once mutations are found in each of the six zebrafish genes whose ventral expression requires *suc/et-1,* these genes can be ordered into genetic pathways by examining the time course of expression of the other ventral arch markers in each mutant. Furthermore, by examining the mutant phenotypes, the specific functional requirements of each of these genes for craniofacial development can be determined.

### Neural crest specification and the timing of *suc/et-1* function in the arches

The ability of *suc/et-1* mutant neural crest cells to adopt ventral arch fates (e.g. express *dHAND* or *EphA3* or contribute to normal ventral cartilages) in a wild-type host shows that the defects in *suc/et-1* mutant neural crest cells are nonautonomous. Our results show that, beginning at approximately 12 hours, transplanted *suc/et-1* mutant neural crest cells migrate into the arches of a wild-type host, mixing extensively with host cells. Thus, *suc/et-1* is not required in neural crest cells for their ventral migration. Furthermore, markers of premigratory and migratory neural crest are unaffected in *suc/et-1* mutant embryos, and injections of human ET-1 protein into arch primordia rescue defects in *suc/et-1* mutant embryos. Therefore, *suc/et-1* appears to function after neural crest migration, to specify ventral fates in the postmigratory arch primordia. Similarly, since the *EdnrA* mutant mice also lack defects in markers of migratory neural crest, Clouthier et al. (2000) conclude that *EdnrA* is required not for neural crest cell migration, but for postmigratory fates. This later requirement for *Et-1/EdnrA* function at a postmigratory stage contrasts to the earlier role of *EdnrB* in neural crest migration demonstrated in mouse embryos by Shin et al. (1999).

### Mosaics, *suc/et-1* expression and later mesodermal and endodermal defects suggest multiple tissue interactions during arch development

Transplants of wild-type mesendodermal cells fail to rescue the *suc/et-1* mutant phenotype, indicating that either small numbers of transplanted wild-type mesendodermal cells are not sufficient to induce ventral markers or rescue cartilage or alternatively, the surface ectoderm domain of *suc/et-1* expression is required for ventral arch fates. Tissue-specific promoters that drive *suc/et-1* expression in one or a subset of its expression domains could be used to assay which *suc/et-1*-expressing tissues control craniofacial development.

Conversely, the ability of *suc/et-1* mutant mesodermal cells to contribute to normal ventral muscles (which are mispatterned in *suc/et-1* mutants) of a wild-type host suggests that paraxial mesoderm does not autonomously require *suc/et-1* for the abililty to form normal ventral muscles. To explain this, we propose bidirectional signaling occurs during arch development. First, Et-1 in the postmigratory neural crest environment specifies ventral arch neural crest fates. Later,

neural crest-derived cells signal back to the paraxial mesoderm to allow correct formation of ventral muscles. This signal would be independent of Et-1, since neural crest does not express *et-1* (Maemura et al., 1996; Clouthier et al., 1998; Nataf et al., 1998; this paper). Consistent with this, *EdnrA* is not expressed in arch paraxial mesoderm in mice and chicks (Clouthier et al., 1998; Kempf et al., 1998; Nataf et al., 1998). Likewise, the endodermal defect in *suc/et-1* mutants suggests a similar *suc/et-1*-dependent feedback to the hyomandibular pouch, a tissue that in mice and chicks does not express *EdnrA* (Clouthier et al., 1998; Kempf et al., 1998; Nataf et al., 1998). In this model, both arch mesodermal and endodermal defects in *suc/et-1* mutants are secondary to earlier defects in neural crest specification. However, the specificity of both the mesodermal and endodermal defects in *suc/et-1* mutants suggests that these defects are revealing specific intertissue signaling events, ultimately dependent on *suc/et-1* and required for proper pharyngeal arch development.

### Potential implications for arch evolution

Our findings, combined with the pharmacological inhibition of the avian EDNRA receptor (Kempf et al., 1998) and the *Et-1/EdnrA/Ece-1* mutant mice (Kurihara et al., 1994; Clouthier et al., 1998; Yanagisawa et al., 1998) suggest that *Et-1*'s requirement for jaw development is evolutionarily ancient and dates back to the common ancestor of teleosts and amniotes. Perhaps recruitment or modification of *et-1* signaling in the anterior arches of agnathans played a role in the appearance of jaws during evolution. Examining expression of *et-1* signaling components, and other genes like *dlx*, *msx* and *dHAND* in lamprey anterior arches, could shed light on the homologies of agnathan skeletal elements and hence on jaw evolution itself.

We thank Angel Amores and Bruce Draper for generously providing PAC DNA pools; Yan-Ling Wang for DNA sequencing; John Postlethwait, Don Kane, and Rachel Warga for mapping advice; Hervé Kempf, Dave Raible, and Debbie Yelon for helpful discussions, and Bruce Draper, Bill Jackman, and Lisa Maves for critical reading of the manuscript. This research was supported by NIH grants HS17963 and HD22486. C. T. M. was supported by an NSF predoctoral fellowship and NIH 5-T32-HD07348, T. F. S. was supported by the HFSP and the Wellcome Trust (RCDF 055120), K. H.-L. was supported by NIH grant K08 HL03371, and J. P. was supported by a HHMI summer research fellowship.

## REFERENCES

**Akimenko, M., Ekker, M., Wegner, J., Lin, W. and Westerfield, M.** (1994). Combinatorial expression of three zebrafish genes related to *Distal-less*: part of a homeobox gene code for the head. *J. Neurosci.* **14**, 3475-3486.

**Almasan, A., Mangelsdorf, D. J., Ong, E. S., Wahl, G. M. and Evans, R. M.** (1994). Chromosomal localization of the human retinoid x receptors. *Genomics* **20**, 397-403.

**Amemiya, C. T. and Zon, L. I.** (1999). Generation of a zebrafish P1 artificial chromosome library. *Genomics* **58**, 211-213.

**Amores, A., Force, A., Yan, Y.-L., Joly, L., Amemiya, C., Fritz, A., Ho, R. K., Langeland, J., Prince, V., Wang, Y.-L. et al. (**1998). Zebrafish *hox* clusters and vertebrate genome evolution. *Science* **282**, 1711-1714.

**Angelo, S., Lohr, J., Lee, K. H., Ticho, B., Breitbart, R., Hill, S., Yost, J. and Srivastava, D.** (2000). Conservation of sequence and expression of Xenopus and zebrafish *dHAND* during cardiac, branchial arch and lateral mesoderm development. *Mech. Dev.* (in press).

**Auffray, C., Kuo, J., DeMars, R., Strominger, J. L.** (1983). A minimum of four human class II alpha-chain genes are encoded in the HLA region of chromosome 6. *Nature* **304**, 174-177.

**Bulfone, A., Kim, H.-J., Puelles, L., Porteus, M. H., Grippo, J. F. and Rubenstein, J. L. R.** (1993). The mouse *Dlx-2* (*Tes-1*) gene is expressed in spatially restricted domains of the forebrain, face and limbs in midgestation mouse embryos. *Mech. Dev.* **40**, 129-140.

**Chomczynski, P. and Sacchi, N.** (1987). Single-step method of RNA isolation by acid guanidinium thiocyanate-phenol-chloroform extraction. *Anal. Biochem.* **162**, 156-159.

**Clouthier, D. E., Hosoda, K., Richardson, J. A., Williams, S. C., Yanagisawa, H., Kuwaki, T., Kumada, M., Hammer, R. E. and Yanagisawa, M.** (1998). Cranial and cardiac neural crest defects in endothelin-A receptor-deficient mice. *Development* **125**, 813-824.

**Clouthier, D. E., Williams, S. C., Yanagisawa, H., Wieduwilt, M., Richardson, J. A. and Yanagisawa, M.** (2000). Signaling pathways crucial for craniofacial development revealed by endothelin-A receptor-deficient mice. *Dev. Biol.* **217**, 10-24.

**Edgeworth, F.H.** (1935). *The Cranial Muscles of Vertebrates*. Cambridge: Cambridge University Press.

**Edwards, Y. H., Putt, W., Lekoape, K. M., Stott, D., Fox, M., Hopkinson, D. A., Sowden, J.** (1996). The human homolog T of the mouse T (Brachyury) gene; gene structure, cDNA sequence, and assignment to chromosome 6q27. *Genome Res.* **6**, 226-233.

**Ekker, M., Akimenko, M.-A., Allende, M. L., Smith, R., Drouin, G., Langille, R. M., Weinberg, E. S. and Westerfield, M.** (1997). Relationships among *msx* gene structure and function in zebrafish and other vertebrates. *Mol. Biol. Evol.* **14**, 1008-1022.

**Gates, M. A., Kim, L., Egan, E.S., Cardozo, T., Sirotkin, H. I., Dougan, S. T., Lashkari, D., Abagyan, R., Schier, A. F. and Talbot, W. S.** (1999). A genetic linkage map for zebrafish: comparative analysis and localization of genes and expressed sequences. *Genome Res.* **9**, 334-347.

**Gaunt, S. J., Blum, M. and De Robertis, E. M.** (1993). Expression of the mouse *goosecoid* gene during mid-embryogenesis may mark mesenchymal cell lineages in the developing head, limbs and body wall. *Development* **117**, 769-778.

**Hacker, A. and Guthrie, S**. (1998). A distinct developmental programme for the cranial paraxial mesoderm of the chick embryo. *Development* **125**, 3461-3472.

**Hall, B.** (1978). *Developmental and Cellular Skeletal Biology*. New York: Academic Press, Inc.

**Hatta, K., Schilling, T. F., BreMiller, R. A. and Kimmel, C. B.** (1990). Specification of jaw muscle identity in zebrafish: correlation with *engrailed*-homeoprotein expression. *Science* **250**, 802-805.

**Hauptmann, G. and Gerster, T.** (1994). Two-color whole-mount in situ hybridization to vertebrate and Drosophila embryos. *Trends Gen.* **10**, 266.

**Hoehe, M. R., Ehrenreich, H., Otterud, B., Caenazzo, L., Plaetke R., Zander, H., Leppert, M.** (1993). The human endothelin-1 gene (EDN1) encoding a peptide with potent vasoactive properties maps distal to HLA on chromosome arm 6p in close linkage to D6S89. *Cytogenet. Cell Genet.* **62**, 131-135.

**Holder, N. and Klein, R.** (1999). Eph receptors and ephrins: effector molecules of morphogenesis. *Development* **126**, 2033-2044.

**Janes, R. W., Peapus, D. H. and Wallace, B. A.** (1994). The crystal structure of human endothelin. *Nat. Struct. Biol.* **1**, 311-319.

**Johnson, S. L., Midson, C. N., Ballinger, E. W. and Postlethwait, J. H.** (1994). Identification of RAPD primers that reveal extensive polymorphism between laboratory strains of zebrafish. *Genomics* **19**, 152-156.

**Johnson, S. L., Gates, M. A., Johnson, M., Talbot, W. S., Horne, S., Baik, K., Rude, S., Wong, J. R. and Postlethwait, J. H.** (1996). Centromere-linkage analysis and consolidation of the zebrafish genetic map. *Genetics* **142**, 1277-1288.

**Jowett, T. and Lettice, L.** (1994). Whole-mount in situ hybridizations on zebrafish embryos using a mixture of digoxygenin- and fluorescein-labelled probes. *Trends Genet.* **10**, 73-73.

**Kempf, H., Linares, C., Corvol, P. and Gasc, J.-M.** (1998). Pharmacological inactivation of the endothelin type A receptor in the early chick embryo: a model of mispatterning of the branchial arch derivatives. *Development* **125**, 4931-4941.

**Kilpatrick, T. J., Brown, A., Lai, C., Gassmann, M., Goulding, M. and Lemke, G.** (1996). Expression of the *Tyro4/Mek4/Cek4* gene specifically marks a subset of embryonic motor neurons and their muscle targets. *Mol. Cell. Neurosci.* **7**, 62-74.

**Kimmel, C. B., Warga, R. M. and Schilling, T. F.** (1990). Origin and organization of the zebrafish fate map. *Development* **108**, 581-594.

**Kimmel, C. B., Ballard, W. W., Kimmel, S. R., Ullmann, B. and Schilling, T. F.** (1995). Stages of embryonic development of the zebrafish. *Dev. Dyn.* **203**, 253-310.

**Kimmel, C. B., Miller, C. T., Kruze, G., Ullmann, B., BreMiller, R. A.,**

**Larison, K. D., Snyder, H. C.** (1998). The shaping of pharyngeal cartilages during early development of the zebrafish. *Dev. Biol.* **203**, 245-263.

**Knapik, E. W., Goodman, A., Ekker, M., Chevrette, M., Delgado, J., Neuhauss, S., Shimoda, N., Driever, W., Fishman, M. C. and Jacob, H. J. (**1998). A microsatellite genetic linkage map for zebrafish (*Danio rerio*). *Nat. Genet.* **18**, 338-343.

**Kollar, E. J. and Mina, M.** (1991). Role of the early epithelium in the patterning of the teeth and Meckel's cartilage. *J. Craniofac. Genet. Dev. Biol.* **11**, 223-228.

**Köntges, G. and Lumsden, A.** (1996). Rhombencephalic neural crest segmentation is preserved throughout craniofacial ontogeny. *Development* **122**, 3229-3242.

**Krauss, S., Concordet, J.-P. and Ingham, P. W.** (1993). A functionally conserved homolog of the Drosophila segment polarity gene *hh* is expressed in tissues with polarizing activity in zebrafish embryos. *Cell* **75**, 1431-1444.

**Kroll, K. L. and Amaya, E.** (1996). Transgenic *Xenopus* embryos from sperm nuclear transplantations reveal FGF signaling requirements during gastrulation. *Development* **122**, 3173-3183.

**Kula, K., Hall, K., Hart, T., Wright, J. T.** (1996). Craniofacial morpohology of the tricho-dento-osseous syndrome. *Clin. Genet.* **50**, 446-454.

**Kurihara, Y., Kurihara, H., Suzuki, H., Kodama, T., Maemura, K., Nagai, R., Oda, H., Kuwaki, T., Cao, W.-H., Kamada, N. et. al. (**1994). Elevated blood pressure and craniofacial abnormalities in mice deficient in endothelin-1. *Nature* **368**, 703-710.

**Maemura, K., Kurihara, H., Kurihara, Y., Oda, H., Ishikawa, T., Copeland, N. G., Gilbert D. J., Jenkins, N. A. and Yazaki, Y.** (1996). Sequence analysis, chromosomal location, and developmental expression of the mouse preproendothelin-1 gene. *Genomics* **31**, 177-184.

**Mallatt, J.** (1997). Crossing a major morphological boundary: The origin of jaws in vertebrates. *Zoology* **100**, 128-140.

**Mina, M., Upholt, W. B. and Kollar, E. J.** (1994). Enhancement of avian mandibular chondrogenesis in vitro in the absence of epithelium. *Arch. Oral Biol.* **39**, 551-562.

**Miyake, T., McEachran, J. D. and Hall, B. K.** (1992). Edgeworth's legacy of cranial muscle development with an analysis of muscles in the ventral gill arch region of batoid fishes (Chondricthyes: Batoidea). *J. Morph.* **212**, 213-256.

**Moens, C.B. and Fritz, A.** (1999). Techniques in neural development. *Methods Cell Biol.* **59**, 253-272.

**Morasso, M. I., Grinberg, A., Robinson, G., Sargent, T. D. and Mahon, K. A.** (1999). Placental failure in mice lacking the homeobox gene *Dlx3*. *Proc. Natl. Acad. Sci. USA* **96**, 162-167.

**Nataf, V., Grapin-Botton, A., Champeval, D., Amemiya, A., Yanagisawa, M. and LeDouarin, N. M.** (1998). The expression pattern of endothlin-A receptor and endothelin-1 in the avian embryo. *Mech. Dev.* **75**, 145-149.

**Noden, D. M.** (1983a). The role of the neural crest in patterning of avian cranial skeletal, connective, and muscle tissues. *Dev. Biol.* **96**, 144-165.

**Noden, D. M.** (1983b). The embryonic origins of avian cephalic and cervical muscles and associated connective tissues. *Am. J. Anat.* **168**, 257-276.

**Odenthal, J. and Nüsslein-Volhard, C.** (1998). *fork head* domain genes in zebrafish. *Dev., Genes, and Evol.* **208**, 245-258.

**Piotrowski, T., Schilling, T. F., Brand, M., Jiang, Y.-J., Heisenberg, C.-P., Beuchle, D., Grandel, H., van Eeden, F. J. M., Furutani-Seiki, M., Granato, M. et al. (**1996). Jaw and branchial arch mutants in zebrafish II: anterior arches and cartilage differentiation. *Development* **123**, 345-356.

**Postlethwait, J. H., Yan, Y.-L., Gates, M. A., Horne, S., Amores, A., Brownlie, A., Donovan, A., Egan, E. S., Force, A., Gong, Z. et al. (**1998). Vertebrate genome evolution and the zebrafish gene map. *Nat. Genet.* **18**, 345-349.

**Price, J. A., Bowden, D. W., Wright, J. T., Pettenati, M. J. and Hart, T. C.** (1998). Identification of a mutation in DLX3 associated with tricho-dento-osseous (TDO) syndrome. *Hum. Mol. Genet.* **7**, 563-569.

**Qiu, M., Bulfone, A., Martinez, S., Meneses, J. J., Shimamura, K., Pederson, R. A. and Rubenstein, J. L. R.** (1995). Null mutation of *Dlx-2* results in abnormal morphogenesis of proximal first and second branchial arch derivatives and abnormal differentiation in the forebrain. *Genes Dev.* **9**, 2523-2538.

**Qiu, M., Bulfone, A., Ghattas, I., Meneses, J. J., Christensen, L., Sharpe, P. T., Presley, R., Pederson, R. A. and Rubenstein, J. L. R.** (1997). Role of the Dlx homeobox genes in proximodistal patterning of the branchial arches: mutations of Dlx-1, Dlx-2, and Dlx-1 and -2 alter morphogenesis of proximal skeletal and soft tissue structures derived from the first and second arches. *Dev. Biol.* **185**, 165-184.

**Rivera-Perez, J. A., Mallo, M., Gendron-Maguire, M., Gridley, T. and Behringer, R. R.** (1995). *goosecoid* is not an essential component of the mouse gastrula organizer but is required for craniofacial and rib development. *Development* **121**, 3005-3012.

**Robinson, G. W. and Mahon, K. A.** (1994). Differential and overlapping expression domains of *Dlx-2* and *Dlx-3* suggest distinct roles for *Distal-less* homeobox genes in craniofacial development. *Mech. Dev.* **48**, 199-215.

**Satokata, I. and Maas, R.** (1994). *Msx1* deficient mice exhibit cleft palate and abnormalities of craniofacial and tooth development. *Nat. Genet.* **6**, 348-356.

**Schilling, T. F. and Kimmel, C. B.** (1994). Segment and cell type lineage restrictions during pharyngeal arch development in the zebrafish embryo. *Development* **120**, 483-494.

**Schilling, T. F., Walker, C. and Kimmel, C. B.** (1996). The *chinless* mutation and neural crest interactions in zebrafish jaw development. *Development* **122**, 1417-1426.

**Schilling, T. F. and Kimmel, C. B.** (1997). Musculoskeletal patterning in the pharyngeal segments of the zebrafish embryo. *Development* **124**, 2945-2960.

**Schilling, T. F.** (1997). Genetic analysis of craniofacial development in the vertebrate embryo. *BioEssays* **19**, 459-468.

**Schulte-Merker, S., Hammerschmidt, M., Beuchle, D., Cho, K. W., De Robertis, E. M. and Nüsslein-Volhard, C.** (1994). Expression of zebrafish *goosecoid* and *no tail* gene products in wild-type and mutant *no tail* embryos. *Development* **120**, 843-852.

**Shin, M. K., Levorse, J. M., Ingram, R. S. and Tilghman, S. M.** (1999). The temporal requirement for endothelin receptor-B signalling during neural crest development. *Nature* **402**, 496-501.

**Storm, E. E. and Kingsley, D. M.** (1996). Joint patterning defects caused by single and double mutations in members of the bone morphogenetic protein (BMP) family. *Development*, **122**, 3969-3979.

**Streisinger, G., Walker, C., Dower, N., Knauber, D. and Singer, F.** (1981). Production of clones of homozygous diploid zebra fish (*Brachydanio rerio*). *Nature* **291**, 293-296.

**Streisinger, G., Singer, F., Walker, C., Knauber, D. and Dower, N.** (1986). Segregation analyses and gene-centromere distances in zebrafish. *Genetics* **112**, 311-319.

**Tam, J. P., Liu, W., Zhang, J. W., Galantino, M., Bertolero, F., Cristiani, C., Vaghi, F., de Castiglione, R.** (1994). Alanine scan of endothelin: importance of aromatic residues. *Peptides* **15**, 703-708.

**Thisse, C., Thisse, B., Schilling, T.F. and Postlethwait, J. H.** (1993). Structure of the zebrafish *snail1* gene and its expression in wild-type, *spadetail* and *no tail* mutant embryos. *Development* **119**, 1203-1215.

**Thisse, C., Thisse, B. and Postlethwait, J. H.** (1995). Expression of *snail2*, a second member of zebrafish snail family, in cephalic mesendoderm and presumptive neural crest of wild-type and *spadetail* mutant embryos. *Dev. Biol.* **172**, 86-99.

**Thomas, T., Kurihara, H., Yamagishi, H., Kurihara, Y., Yazaki, Y., Olson, E. N. and Srivastava, D.** (1998). A signaling cascade involving *endothelin-1*, *dHAND*, and *Msx1* regulates development of neural-crest-derived branchial arch mesenchyme. *Development* **125**, 3005-3014.

**Trainor, P. A., Tan, S-S. and Tam, P. P. L.** (1994). Cranial paraxial mesoderm: regionalisation of cell fate and impact on craniofacial development in mouse embryos. *Development* **120**, 2397-2408.

**Trainor, P. A. and Tam, P. P. L.** (1995). Cranial paraxial mesoderm and neural crest cells of the mouse embryo: co-distribution in the craniofacial mesenchyme but distinct segregation in branchial arches. *Development* **121**, 2569-2583.

**Weinberg E. S., Allende M. L., Kelly C. S., Abdelhamid A., Murakami T., Andermann P., Doerre O. G., Grunwald D. J. and Riggleman B.** (1996). Developmental regulation of zebrafish *MyoD* in wild-type, *no tail* and *spadetail* embryos. *Development* **122**, 271-280.

**Westerfield, M., Wegner, J., Jegalian, B. G., DeRobertis, E. M. and Püschel, A. W.** (1992). Specific activation of mammalian *Hox* promoters in mosaic transgenic zebrafish. *Genes Dev.* **6**, 591-598.

**Westerfield, M.** (1995). *The Zebrafish Book.* University of Oregon; Eugene, OR.

**Xu, Q., Holder, N., Patient, R., Wilson, S. W.** (1994). Spatially regulated expression of three receptor tyrosine kinase genes during gastrulation in the zebrafish. *Development* **120**, 287-299.

**Yamada, G., Mansouri, A., Torres, M., Stuart, E. T., Blum, M., Schultz, M., De Robertis, E. M. and Gruss, P.** (1995). Targeted mutation of the murine *goosecoid* gene results in craniofacial defects and neonatal death. *Development* **121**, 2917-2922.

**Yanagisawa, H., Yanagisawa, M., Kapur, R. P., Richardson, J. A., Williams, S. C., Clouthier, D. E., de Wit, D., Emoto, N. and Hammer, R. E.** (1998). Dual genetic pathways of endothelin-mediated intercellular signaling revealed by targeted disruption of endothelin converting enzyme-1 gene. *Development* **125**, 825-836.